INTEGRATED TRANSCRIPTOMIC AND PROTEOMIC ANALYSIS REVEALS ROLE OF THE HEXOSAMINE BIOSYNTHETIC PATHWAY IN INVASION AND METASTASIS OF HEPATOCELLULAR CARCINOMA

by
Christine Lam

A dissertation submitted to Johns Hopkins University in conformity with the requirements for the degree of Doctor of Philosophy

Baltimore, Maryland
August 2021

Abstract

Hepatocellular carcinoma (HCC) is a major global cause of mortality. The epithelial-mesenchymal transition (EMT) transcription factor TWIST1 has been implicated in the invasion and metastasis of HCC, but the mechanism is unclear. My goal was to define a cancer cell autonomous mechanism of Twist1-induced metastasis in HCC. Integrated transcriptomic and proteomic analyses on primary liver tumors and lung metastases from a spontaneous *Twist1*-dependent metastasis mouse model of *MYC*-induced HCC identified the hexosamine biosynthetic pathway (HBP) as a cancer cell autonomous mechanism for EMT-mediated invasion and metastasis. I demonstrated that the hexosamine biosynthetic pathway is required and sufficient for invasion and metastasis *in vitro* in HCC cell lines, *ex vivo* in HCC tumor-derived organoids, and *in vivo* in a genetically engineered mouse model of metastatic HCC. Therefore, the HBP may be a potential therapeutic target for advanced HCC patients.

Readers

Phuoc T. Tran, M.D., Ph.D.

Fred Bunz, M.D., Ph.D.

Dissertation Committee

Phuoc T. Tran, M.D., Ph.D. (Principal Investigator)

Fred Bunz, M.D., Ph.D. (Chair)

Dean Felsher, M.D., Ph.D.

Robert Anders, M.D.

Acknowledgements

First and foremost, I would like to thank my PhD thesis advisor, Phuoc Tran. He has been an incredible mentor, both professionally and personally.

My PhD would not have been possible without my family. As immigrants without an education, my parents worked difficult jobs in construction and food service to support my dreams. It is truly a privilege to be the first in my family to graduate university and complete a PhD. It has been a blessing to have a sister who is also pursuing a PhD on the East Coast. I am grateful for my many New York City adventures with Nora.

I would like to thank my labmates in the Tran Lab. Audrey Lafargue has been like an older sister figure to me; she has been incredibly supportive through the most difficult times. Hailun Wang has been an amazing mentor and resource for training in lab techniques; our scientific discussions have added valuable insight into my work, and I am thankful for the time he has spent teaching me various techniques. My interactions with each and every member of the Tran Lab has helped me; they have re-charged me during challenging days and helped me with my research.

My friends have been instrumental to my PhD, and I am extremely grateful for their support over the years. They have made my good days great and my bad days okay. They have been the best support system these past four years, and I could not have done it without them.

TABLE OF CONTENTS

LIST OF FIGURES

<u>Chapter 1</u>: Background and relevant literature

<u>Chapter 2</u>: Defining the EMT-HBP-O-GlcNAcylation axis as a cancer cell-autonomous mechanism for Twist1-induced metastasis in hepatocellular carcinoma

Chapter 1: Background and relevant literature

1.1 Introduction

Epithelial plasticity (EP) programs such as the epithelial-mesenchymal transition (EMT) and mesenchymal-epithelial transition (MET) are evolutionarily conserved processes that are essential for embryonic development. EP also plays an important role during tumor progression toward metastasis and treatment resistance, and new roles in the acceleration of tumorigenesis have been found. Recent evidence has linked EMT-related transcriptomic alterations with metabolic reprogramming in cancer cells, which include increased aerobic glycolysis. More recent studies have revealed a novel connection between EMT and altered glycosylation in tumor cells, in which EMT drives an increase in glucose uptake and flux into the hexosamine biosynthetic pathway (HBP.)

The HBP is a side-branch pathway from glycolysis that generates the end product uridine-5′-diphosphate-N-acetylglucosamine (UDP-GlcNAc.) UDP-GlcNAc is covalently added to protein substrates as the post-translational modification known as O-GlcNAcylation, in which the GlcNAc moiety is linked to Ser/Thr/Asn residues. Global changes in protein O-GlcNAcylation are emerging as a general characteristic of cancer cells. In our recent study, we demonstrated that the EMT-HBP-O-GlcNAcylation axis drives the O-GlcNAcylation of key proteins such as c-Myc, which previous studies have shown to suppress oncogene-induced senescence (OIS) and contribute to accelerated tumorigenesis. Here, I review the HBP and O-GlcNAcylation and their putative roles in driving EMT-related cancer processes with examples to illuminate potential new therapeutic targets for cancer.

1.2 Epithelial plasticity: Basics and implications in cancer development, progression, and treatment resistance

Epithelial plasticity (EP) programs such as the epithelial-mesenchymal transition (EMT) and the reverse mesenchymal-epithelial transition (MET) are developmental programs that can engender cells with a fluid cellular phenotype that span fully epithelial to fully mesenchymal properties and potentially many hybrid states in-between (Figure 1.1.) EP programs are well-conserved, essential for normal development and can be reactivated by some cancer cells (Chaffer & Weinberg, 2011.)

The EMT has been studied in detail. During this process epithelial cells undergo a transcriptional and resultant biochemical change that confers a more mesenchymal phenotype. Extracellular signaling mediated by TGF-β, receptor tyrosine kinases (RTKs,) integrins, WNT, NOTCH, Hedgehog (HH,) hypoxia inducible factor 1α (HIF1α) and JAK/STAT induce the EMT in various biological contexts (Taparra, Tran, & Zachara, 2016.) Inside cells, canonical EMT is mainly executed by three major families of EMT-inducing transcription factors (TFs): the zinc finger protein Snail family (SNAI1, SNAI2, and SNAI3); the zinc finger E-box binding (ZEB) family; and basic Helix-Loop-Helix (bHLH) proteins (TWIST1 and TWIST2) (Nieto, Huang, Jackson, & Thiery, 2016.) These EMT-TFs in general lead to the downregulation of epithelial genes and upregulation of mesenchymal genes, resulting in the loss of cellular adhesion, loss of cell polarity, and reorganization of the cytoskeleton (Carvalho-Cruz, Alisson-Silva, Todeschini, & Dias, 2018.) Some canonical markers for this transition are the loss of the epithelial adhesion protein E-cadherin, ZO-1, and cytokeratins and replacement by N-Cadherin, fibronectin, and vimentin. Additional defining cellular phenotypes include a more

migratory, stress/death-resistant behavior, immune evasive and neoplastic-prone state of these cells (Dongre et al., 2017; Nieto et al., 2016.)
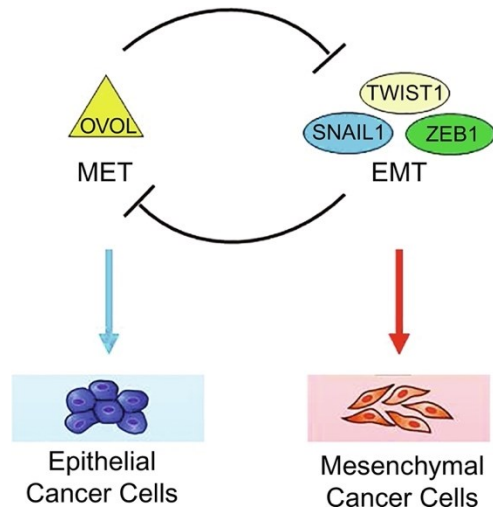
Figure 1.1 Model of epithelial plasticity involving EMT-MET balance in human cancer.

In human cancer cells the mesenchymal and epithelial states are induced and maintained by transcriptional and post-transcriptional regulatory programs. These programs are controlled by the feedback regulation between the OVOL and EMT-inducing TFs such as Zeb1, Twist1 and Snail1, critical inducers of MET and EMT respectively. Therefore high OVOL and low EMT-TFs stabilize the epithelial state decreasing cancer cell invasion and metastasis, and vice versa for the mesenchymal state.

1.3 Cancer metabolism: Metabolic adaptations in cancer

Altered metabolism is one of the hallmarks of cancer. The best-known metabolic anomaly in cancers is an increase in aerobic glycolysis, which generates ATP and other basic

3

building blocks, such as nucleotides, lipids, and proteins to support tumor cell growth and survival.

Early investigation into tumor metabolism was based on the observation that cancer cells grow very rapidly and in a disorganized manner, thereby setting them apart from either the rapidly proliferative but highly organized cells of normal development or the relatively less active normal epithelia (Warburg, 1925.) Warburg and colleagues observed that, contrary to their expectation, carcinoma tissue exhibited levels of respiration lower than normal kidney or liver tissue, but underwent anaerobic glycolysis, the transformation of simple sugars to lactic acid in the absence of oxygen, at a rate many-fold higher than normal tissues. Subsequently, they observed that carcinoma tissue maintains significant rates of glycolysis even under aerobic conditions, while normal tissues do not. In a follow-up publication, Warburg et al. showed that carcinoma cells could survive not only under anaerobic conditions permitting glycolysis, but not respiration, and also when deprived of glucose under aerobic conditions, but not in circumstances precluding both glycolysis and respiration concurrently (Warburg, Wind, & Negelein, 1927.) These findings set the stage for investigation into whether the upregulation of glycolysis is merely to ensure energy production during oxygen stress, or if this metabolic derangement provides additional selective advantages to cancer cells.

The initial result of glycolysis is the conversion of a single molecule of glucose into 2 of pyruvate, a net increase of 2 ATP, and the reduction of 2 NAD + to NADH. The subsequent fate of pyruvate varies based on environmental factors, most importantly in the presence of oxygen: pyruvate can be converted anaerobically into lactate ("anaerobic glycolysis") or aerobically into acetyl-CoA which can then proceed through the citric acid cycle and fuel

mitochondrial oxidative phosphorylation. Energetically, anaerobic glycolysis results in a redox-neutral production of 2 ATP, while progression through oxidative phosphorylation ultimately produces 30–32 ATP per glucose consumed; it is this latter process that typically predominates in normal human tissues. The "aerobic glycolysis" described by Warburg and colleagues refers not to a unique process, but rather a tendency of cancer cells (or other rapidly proliferative cells) to convert large amounts of pyruvate to lactate anaerobically even in the presence of oxygen.

Decades of debate and investigation were spent asking whether this shift toward glycolysis was because tumors cannot appropriately utilize oxidative phosphorylation due to mitochondrial dysfunction, or if the biosynthetic benefits of glycolysis balance out the significant energetic sacrifices incurred. Ultimately the latter assertion appears most consistent with our collective understanding of tumor biology. While fewer ATP molecules are generated per glucose molecule than would otherwise be generated through oxidative phosphorylation, the conversion of pyruvate to lactate can lead to faster ATP production and NAD + regeneration than oxidative phosphorylation (Guppy, Greiner, & Brand, 1993.) Maintenance of a sufficient intracellular glucose pool to fuel glycolysis is achieved by significant upregulation of glucose transporters by tumor cells (Labak et al., 2016,) a phenomenon which is evident in the broad diagnostic utility of positron emission tomography (PET) imaging using ^{18}F-fluorodeoxyglucose (^{18}F-FDG) in cancer detection. Additionally, tumor upregulation of enzymes involved in gluconeogenesis, the production of glucose from smaller organic molecules which can be broadly conceptualized as "reverse glycolysis," provides an important mechanism for maintaining glucose pools. In principle, "reverse glycolysis" may be particularly relevant to areas in the body which are poorly perfused and thus less able to scavenge glucose from the

bloodstream (Leithner et al., 2015.) Furthermore, a tumor requires not just energy, but all of the building blocks necessary for growth (Vander Heiden, Cantley, & Thompson, 2009.)

Far beyond glycolysis, there is a large body of literature describing how oncogenes and tumor suppressor genes commonly implicated in tumorigenesis modify the bioenergetics of cancer cells to promote anabolism necessary for rapid growth proliferation (Jones & Thompson, 2009.) Upregulation of c-Myc leads to increased aerobic glycolysis by increasing lactate dehydrogenase (LDH-A) activity (Osthus et al., 2000,) as well as increased nucleotide and amino acid metabolism (Gordan, Thompson, & Simon, 2007.) The pentose phosphate pathway, also known as the phosphogluconate pathway (or hexose monophosphate shunt,) metabolizes glucose-6-phosphate to ribulose-5-phosphate, a precursor of ribonucleotide synthesis, while generating reduced nicotinamide adenine dinucleotide phosphate (NADPH,) critical for maintenance of cellular redox balance and a component of several anabolic pathways (Kowalik, Columbano, & Perra, 2017.) These products are vitally important to highly proliferative cells and several of the enzymes in this pathway including glucose-6-phosphate dehydrogenase (G6PD,) 6-phosphogluconate dehydrogenase, transaldolase, and transketolase can be overactive in cancers. Tumor cells are also known to upregulate de novo synthesis of fatty acids, mobilization of fatty acid stores from lipolysis of triglycerides, and uptake of exogenous lipids from their surroundings through increased expression of the fatty acid receptor CD36, low density lipoprotein receptor (LDLr,) and the fatty acid binding proteins FABP4, FABP5, and FABP7 (Liu, Luo, Halim, & Song, 2017.)

More recent evidence links EMT-related transcriptomic alterations with metabolic reprograming in cancer cells, which include increased aerobic glycolysis and the accumulation of dihydropyrimidines (Shaul et al., 2014.) EMT has been implicated in metabolic reprogramming of cancer cells; cancer cells undergoing EMT exhibit aberrant glucose metabolism, but these alterations have yet to be vigorously explored (Morandi, Taddei, Chiarugi, & Giannoni, 2017.) It has been shown previously that cancer cells undergoing EMT increase glucose intake; Liu et al. exposed pancreatic ductal carcinoma (PDAC) cells to the EMT inducers TNFα and TGF-ß and found increased glucose intake and lactate production with no effect on oxidative phosphorylation (OXPHOS) metabolism (Liu, Quek, Sultani, & Turner, 2016.) Dong et al. demonstrated that EMT in breast cancer exhibited glycolysis induction, increased glucose uptake, and inhibition of oxygen consumption (Dong et al., 2013); Kondaveeti et al. also induced EMT in two breast cancer cell lines and found increased glycolysis and decreased gluconeogenesis (Kondaveeti, Guttilla Reed, & White, 2015.) Two recent studies also revealed a novel connection between EMT and altered glycosylation in tumor cells. Lucena et al. demonstrated an increase in glucose uptake and flux into the hexosamine biosynthetic pathway (HBP) during TGF-β-induced EMT in a non-small cell lung cancer (NSCLC) cell line (Lucena et al., 2016.) In addition, Taparra et al. found that EMT elevated levels of key HBP genes in NSCLC mouse models (Taparra et al., 2018.) These studies highlight that glucose metabolism, especially the HBP, may be important metabolic pathways to target in EMT-mediated cancers and will be discussed in greater detail below.

1.4 Glycobiology: An introduction to protein glycosylation and relevance to cancer

Glycosylation is the covalent attachment of oligo- or polysaccharide sugars to other molecules such as proteins to form glycans and glycoproteins. Glycosylation of other macromolecules such as lipids and even other sugars occurs abundantly in nature, but our focus will be on protein glycoconjugates. Glycosylation is one of the most important biological post-translational protein modifications and occurs predominantly in the cytosol, the endoplasmic reticulum, the Golgi apparatus and at the cell membrane. Glycosylation of proteins can substantially influence and modulate protein structure and function and appears to be involved in the fine tuning of cell–cell recognition and cellular signaling processes. Interestingly, altered glycosylation is a universal feature of cancer cells, and has been frequently correlated with malignant transformation and tumor progression. Glycosylations are well positioned to mediate many of the cellular changes associated with cancer, modifying cell-cell adhesion, responsiveness to growth factors, immune system evasion, metabolic adaptation and changes in signal transduction (Varki, Kannagi, Toole, & Stanley, 2015.)

In general, there are two major types of glycosylation that occur on proteins. More commonly carbohydrate moieties can be linked to the amide group of asparagine (N-linkage) or the hydroxyl-containing sidechain of serine or threonine (O-linkage.) N-linked glycosylation is a frequent processing step for proteins bound for the plasma membrane or export from the cell. The initial step takes place within the lumen of the endoplasmic reticulum, where NXS/T motifs (N: asparagine, X: any amino acid but proline, S/T: serine or threonine) are N-glycosylated by oligo-saccharyltransferase (OST,) which transfers a highly conserved

Glc$_3$Man$_9$GlcNAc$_2$ oligosaccharide to the asparagine sidechain of the acceptor motif (Aebi,

2013.) After assembly and conjugation of the core oligosaccharide in the ER, a wide variety of

additional modifications can occur in the Golgi apparatus, including substitution and/or addition

of saccharides moieties as well as creation of higher-order branching structures (Wang et al.,

2017.) The resulting N-linked glycoproteins are classified as high mannose, complex, and

hybrid. The core structure of all N-linked glycoproteins is a chain of two N-

acetylglucosamine (GlcNAc) followed by a branching mannose triad. High mannose N-linked

glycoproteins are typified by additional branching mannose residues beyond the core structure,

while complex N-linked glycoproteins may contain additional carbohydrate moieties including

but certainly not limited to glucose, galactose, fucose, xylose, GlcNAc, N-

acetylgalactosamine, N-acetylneuraminic acid (commonly known as sialic acid,) N-

glycolylneuraminic acid, and glucuronic acid (Costa, Rodrigues, Henriques, Oliveira, &

Azeredo, 2014.) Relevant to this review, many prototypical EP markers are modified by N-

linked glycans such as E-cadherin and N-cadherin which ultimately affect their protein activity

and function resulting in changes in cellular signal transduction, adhesion and migration (Guo,

Lee, Kamar, & Pierce, 2003; Pinho et al., 2009; Zhou et al., 2008.) In addition, N-glycosylation

of cell surface receptors is an important determinant of signaling behavior as the number and

structure of N-glycans on receptors influences their rate of endocytosis (Dennis, Lau, Demetriou,

& Nabi, 2009.) For example, association of N-glycans on unbound receptor tyrosine kinases

with galectins in the plasma membrane restricts lateral diffusion, prevents endocytosis, and

thereby promotes availability for ligand binding, but also serves to prevent ligand-independent

receptor activation and maintain signaling integrity. This concept extends beyond the cell of

origin, as glycosylation also impacts protein interactions with distant cells and, in higher

organisms such as humans, removal of target cells from the circulation (Costa et al., 2014.)

O-linked glycosylation is more variable in its execution than N-linked glycosylation, but

no less important. Among the simplest forms of O-linked glycosylation is the addition of a single

mannose to the hydroxyl of a serine or threonine residue, termed O-mannosylation, appears to be

involved in identification and processing of misfolded proteins within the endoplasmic reticulum

(Loibl & Strahl, 2013.) Conjugation of a single GlcNAc, referred to as O-GlcNAcylation, acts as

a rapidly cycling modification more conceptually akin to phosphorylation than to complex

glycosylation and regulates transcription, translation, and protein trafficking within the nucleus,

cytoplasm and mitochondria (Hart & Akimoto, 2009.) For example, increased O-GlcNAcylation

of G6PD in non-small cell lung cancer promotes growth and proliferation through upregulation

of the pentose phosphate pathway activity (Rao et al., 2015.) O-GlcNAcylation is a unique form

of protein glycosylation that will be discussed in greater detail below. More complex, branching

O-glycans are frequently antigenic, for example the determinants of the ABO and Lewis blood

groups, and are integral to the mucinous glycoproteins found in mucous membrane secretions

(Brockhausen, Schachter, & Stanley, 2009.)

1.5 The hexosamine biosynthetic pathway (HBP): An emerging metabolic player in cancer

The HBP is a side-branch metabolic sensing pathway from glycolysis, in which 2–5% of

total glucose is diverted at the fructose-6-phosphate step. The HBP ultimately converts glucose

to the end product uridine-5′-diphosphate-N-acetylglucosamine (UDP-GlcNAc.) which is critical

for the post-translational modifications of proteins, such as protein glycosylation. Despite the limited flux through the HBP, cellular UDP-GlcNAc is among the most abundant high-energy cellular compounds reaching levels over 1 mM in concentration (Sasai, Ikeda, Fujii, Tsuda, & Taniguchi, 2002.) The first step in the HBP is the transfer of an amide group by glutamine:fructose-6-phosphate amidotransferase (GFAT) from glutamine to fructose-6-phosphate to form glucosamine-6-phosphate (GlcN6P) and glutamate (Figure 1.2) (Marshall, Bacote, & Traxinger, 1991.) This step is rate-limiting for the HBP and the rapid turnover ($t_{1/2}$ = 45 min) allows for rapid adaptation to environmental alterations; furthermore, the action of GFAT is the only known mechanism for production of GlcN-6P. Feedback inhibition of GFAT activity occurs through allosteric binding of UDP-GlcNAc, the terminal product of the HBP, while phosphorylation by protein kinase A (PKA,) AMP-activated protein kinase (AMPK,) and calcium/calmodulin-dependent kinase II (CaMKII) are implicated in upregulation of GFAT activity, thereby potentially linking the HBP to myriad autocrine, paracrine, and endocrine signaling axes including but not limited to cyclic AMP, adrenergic, adiponectin, and receptor tyrosine kinase signaling (Durand, Golinelli-Pimpaneau, Mouilleron, Badet, & Badet-Denisot, 2008.) GFAT activity is also implicated in cytokine synthesis and extracellular matrix interactions (Weigert, Friess, Brodbeck, Haring, & Schleicher, 2003.) Conflicting data exist on the role of GFAT isoenzymes in cancer. GFAT1 is a poor prognostic factor in human gastric carcinoma associated with increased invasive behavior and metastasis (Duan et al., 2016.) Analysis of fresh gastric carcinoma and normal gastric mucosal tissue identified decreased GFAT1 mRNA and protein expression with concurrent decreased GlcNAcylation in a subset of tumors, an observation mirrored in representative cell lines and correlated with clinicopathologic variables for poor prognosis such as vascular invasion, advanced T stage, and both nodal and

11

distal metastasis. Kaplan–Meier analysis showed that in both a single-institution patient cohort

and data from The Cancer Genome Atlas (TCGA,) low GFAT1 expression correlated with

inferior overall survival regardless of clinical stage. Knockdown of GFAT1 or chemical

inhibition of GFAT1 with 6-diazo-5-oxo-1-norleucine in gastric cancer cells increased invasive

behavior and resistance to anoikis, downregulated E-cadherin, increased N-cadherin, vimentin,

and Snail1 expression, and increased TGF-β1 secretion. Overall, these data point to GFAT1 as a

suppressor of EMT in gastric cancer. Alternatively, *GFPT2* overexpression has been shown to be

of prognostic significance in three separate large patient lung adenocarcinoma cohorts for

survival and was associated with metabolic reprogramming of the tumor microenvironment and

EMT (Zhang et al., 2018.)
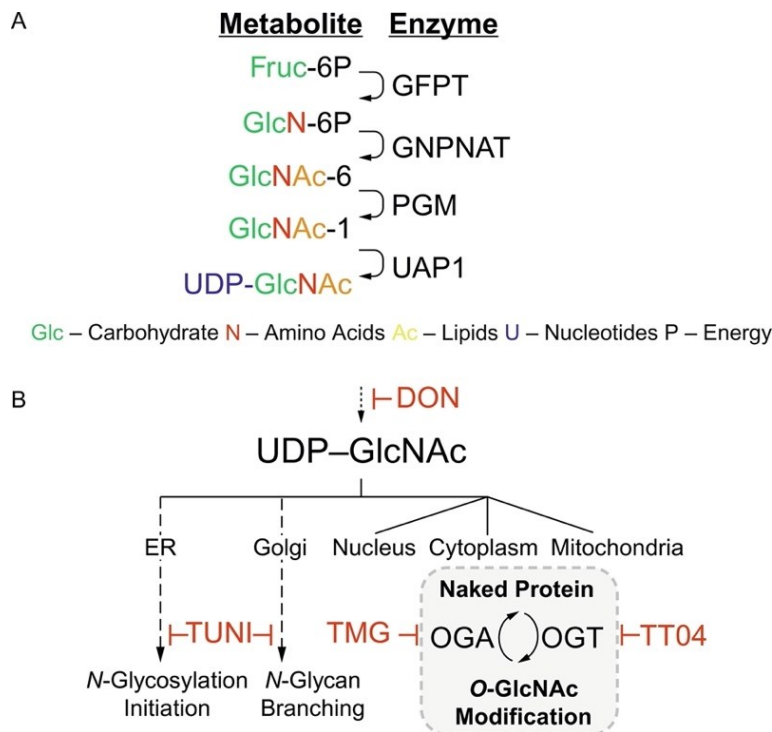
Figure 1.2 The hexosamine biosynthetic pathway.

A) Illustration of the metabolites and enzymatic steps of the HBP pathway. Enzymes: GFAT—glutamine:fructose-6-phosphate amidotransferase; GNPNAT—glucosamine-phosphate N-acetyltransferase; PGM—phosphoacetylglucosamine mutase; and UAP1—UDP-N-acetylhexosamine pyrophosphorylase. Metabolites: Fruc-6P—fructose-6-phosphate; GlcN-6P—glucosamine-6-phosphate; GlcNac-6—N-acetylglucosamine-6-phosphate; GlcNac-1—N-acetylglucosamine-1-phosphate; and UDP-GlcNac—UDP-N-acetyl-glucosamine. B) Schematic showing UDP-GlcNAc incorporation into N-linked and O-linked glycosylation with inhibitors (red.)

Following formation of GlcN6P by GFAT, glucosamine-phosphate N-acetyltransferase (GNPNAT) transfers an acetyl group from acetyl-CoA to GlcN-6P to form N-acetylglucosamine-6-phosphate (GlcNAc-6P) and coenzyme A. An alternative to this step involves lysosomal degradation of glycoproteins to form GlcNAc, which can then be phosphorylated by N-acetylglucosamine kinase to form GlcNAc-6P (Boehmelt et al., 2000.) Loss of activity in the murine ortholog of GNPNAT has been shown to result in reduced proliferation, cell adhesion, and actin depolymerization, as well as resistance to apoptosis (Boehmelt et al., 2000.) These affects appear to be related to defective glycosylation rather than direct action of GNPNAT.

Phosphoacetylglucosamine mutase (PGM3) next transfers the phosphate group of GlcNAac-6P from position 6 to position 1 to form N-acetylglucosamine-1-phosphate (GlcNAc-1P,) requiring Mg^{2+} as a cofactor. PGM3 expression is upregulated in human microvascular endothelial cells in response to erythropoietin, suggesting a role in angiogenesis, again likely

through modulation of interactions between cells and the extracellular matrix (Li, Rodriguez, & Banerjee, 2000.) Congenital mutations resulting in PGM3 loss-of-function lead to glycosylation defects manifesting as decreased CD8 + T-cells and increased production of the T_H2 cytokines IL-4, IL-5, IL-13, and IL-17 by stimulated $CD4^+$ T-cells (Zhang et al., 2014.) A recently described synthetic inhibitor of PGM3 was found to cause significant decreases in tumor proliferation and survival in breast cancer cell lines and mouse xenograft models (Ricciardiello et al., 2018.)

The final step of the HBP is the conjugation of a uridine diphosphate (UDP) moiety to GlcNAc-1P by UDP-N-acetylhexosamine pyrophosphorylase (UAP1) to form UDP-N-acetyl-glucosamine (UDP-GlcNAc.) This process requires uridine triphosphate (UTP) as a reactant, Mg^{2+}/Mn^{2+} as a cofactor, and produces pyrophosphate as a byproduct (Peneff et al., 2001.) UAP1 is also capable of producing UDP-N-acetyl-galactosamine-1-phosphate (UDP-GalNAc) from N-acetyl-galactosamine-1-phosphate (GalNAc-1P,) with the relative affinities of UAP1 for the glucosamine or galactosamine-based species dictated by alternative splicing (Wang-Gillam, Pastuszak, & Elbein, 1998.) UAP1 overexpression has recently been identified in prostate cancer cell lines and appears to protect cells against the growth inhibitory effects of N-linked glycosylation inhibitors (Itkonen et al., 2015.)

UDP-GlcNac is one of the essential carbohydrate building blocks of the $Glc_3Man_9GlcNAc_2$ oligosaccharide transferred during the ER phase of glycosylation (Aebi, 2013.) Subsequent modification of N-glycans in the Golgi apparatus is also dependent on the presence of UDP-GlcNAc and HBP dynamics are tightly linked to cell growth, differentiation, and surface receptor presentation (Lau et al., 2007.) Interestingly, the HBP is well positioned to

serve as a biochemical metabolic barometer for the cell sensing the four macromolecules of life, coordinating carbohydrate, amino acid, lipid, and nucleotide donors through incorporation of Fru-6P, Gln, acetyl-CoA, and uridine, respectively (Wells, Vosseller, & Hart, 2003.) Arguably the most critical downstream utilization of UDP-GlcNAc is the nutrient- and stress-responsive posttranslational modification, O-GlcNAcylation, which involves the attachment of a single GlcNAc moiety to Ser and Thr residues of over 3000 intra-cellular proteins via a β-glycosidic bond (Wells et al., 2003.) In contrast to N-linked glycans, which are controlled by upward of almost two dozen separate enzymes and can be highly branched structures, a single pair of enzymes—O-GlcNAc transferase (OGT) and O-GlcNAcase (OGA)—controls the addition and removal of a single O-GlcNAc (Iyer & Hart, 2003.) O-GlcNAcylation competes with phosphorylation on Ser/Thr and thus regulates diverse cellular processes, which include transcription, protein stability and cell signaling dynamics. Recent studies also support the emerging concept that global changes in protein O-GlcNAcylation is a general characteristic of cancer cells.

1.6 Epithelial plasticity and glycosylations in cancer

1.6.1 Epithelial plasticity and N-linked glycosylations in cancer

Lange-Consiglio et al. investigated the glycobiology of the spontaneous transformation of equine amniotic epithelial cells (AECs) into amniotic mesenchymal cells (AMCs,) which occurs when the former is grown in culture (Lange-Consiglio, Accogli, Cremonesi, & Desantis, 2014.) This transition, referred to as "transdifferentiation" and essentially a form of non-pathologic EMT, was characterized by adoption of an elongated morphology, loss of pan-cytokeratin staining, and gain of vimentin staining. Transdifferentiated cells (termed EMTCs) expressed the

mesenchymal stem-cell markers CD29, CD44, CD166, and CD105, as well as MHC-I. Binding

of a several lectins was quantified in AECs, amniotic mesenchymal cells (AMCs,) and EMTCs

to evaluate glycocalyx composition. EMT upregulated expression of highly mannosylated N-

linked glycans and O-linked sialoglycans with a terminal NeuNAcα2,3Galβ1,3GalNAc moiety,

while downregulating expression of glycans with terminal GlcNAc, fucose, GalNAc,

and galactose. Consistent with the non-pathologic nature of transdifferentiation, EMTCs did not

lose expression of Siaα2-6Gal/GalNAc as has been observed in metastasis-associated EMT.

While these observations collectively support that cells undergoing EMT experience alterations

in their glycosylation profile, clear mechanistic explanations for each of these specific

glycosylation alterations are not yet available.

Li et al. investigated the role of branched N-glycans in TGF-β1-induced EMT in cancer

cells. This group identified the role of Smad signaling in the inhibition of EMT in response to

TGF-β1 and in turn the influence of N-GlcNAcylation on this regulatory mechanism (Li et al.,

2014.) Analysis of patient samples of normal lung epithelium and lung cancers identified lower

N-acetylglucosaminyltransferase V (GnT-V) expression in malignancy (except squamous cell

carcinoma histology) than in normal tissues, and also that GnT-V expression was positively

associated with expression of E-cadherin and negatively associated with N-cadherin and

vimentin, suggesting a correlation between GnT-V expression and a stable epithelial phenotype.

Analysis of normal lung and lung cancer cell lines identified similar trends. In response to TGF-

β1 treatment, known to encourage EMT, A549 cells were found to have lower levels of hybrid

and complex N-linked glycans, particularly those with β1,6-GlcNAc branching structures. TGF-

β1 treatment significantly reduced GnT-V mRNA and protein expression, while chemical

inhibition of β1,6-GlcNAc branched glycan synthesis enhanced the induction of EMT by TGF-β1, as did knockdown of GnT-V by shRNA. Overexpression of GnT-V in A549 cells led to decreased invasiveness and cell migration as well as inhibited EMT in response to TGF-β1, while overexpression of a catalytically inactive GnT-V mutant did not. Further mechanistic investigation found that inhibition of β1,6-GlcNAc branched glycan synthesis or knockdown of GnT-V led to increased Smad2 and Smad3 phosphorylation and nuclear translocation, Smad2/4- and Smad3/4-dependent transcription, and FAK signaling after TGF-β1 treatment. Finally, the overexpression of catalytically active GnT-V led to reciprocal decreases in TGF-β1/Smad signaling. Taken together these results show that TGF-β1 signaling and GnT-V catalysis oppose one another as regulators, positive and negative, respectively, of the EMT in human lung cancer cells.

Khan et al. investigated the role of non-muscle II-A (NMII-A) in a TGF-β1-induced EMT model of NSCLC (Khan et al., 2018.) NMII-A is an actin-binding protein that has a central role in cytokinesis, migration, and adhesion. In this study, the authors induced EMT in a human NSCLC cell line A549 with TGF-β1, and found decreased expression of NMII-A and E-cadherin as well as increased expression of vimentin at the protein level. They also found increased protein expression of JNK and p-JNK, p-SMAD 2/3, and p-P38; upon genetic knockdown of JNK, SMAD 2/3, and P38, TGF-β1 mediated downregulation of NMII-A was inhibited. The authors hypothesized that TGF-β1 regulates the expression of NMII-A via JNK/P38/PI3K pathway. Genetic knockdown of NMII-A in A549 cells resulted in a mesenchymal cell morphology and decreased proliferation, as well as significantly enhanced migration via wound healing assay and transwell assay. NMII-A knockdown cells had decreased protein expression of epithelial markers E-cadherin and ZO1 and increased expression of mesenchymal markers

17

vimentin, N-cadherin, Slug, Snail and β-catenin. The authors then implanted the NMII-A knockdown cells via tail vein injection into mice, and found that NMII-A knockdown cells disseminated to different organs, including the bones, kidney, liver, ovaries, and lungs, and were found at higher levels in the brain. Overall, the NMII-A knockdown cells had enhanced metastasis to brain and bone compared to control cancer cells. Next, they studied these NMII-A knockdown cells in a mouse lung orthotropic model, and found increased metastasis from the left lung injected with cells to the right lung compared to control. The authors found increased vimentin expression in NMII-A knockdown cells in both lungs, as well as decreased E-cadherin expression in NMII-A knockdown cells in the left lung compared to control. Overall, NMII-A knockdown increased tumor metastasis and modified tumor cell distribution *in vivo*.

Next, the authors studied the expression of mucin-type core II beta-1,6-N-acetylglucosaminyltransferase (C2GnT-M) in NMII-A knockdown cells. C2GnT-M is located in the Golgi apparatus; when it binds to the C-terminal region of NMII-A, C2GnT-M is transported to the endoplasmic reticulum, where it is recycled and degraded. In addition, C2GnT-M is responsible for the synthesis of all three branch structures, including core 2, core 4, and I antigen found in the glycans of secreted mucins. These three branch structures are generated by the transfer of GlcNAc from UDP-GlcNAc to core 1, core 3, and I antigen. The authors found increased mRNA and protein levels of C2GnT-M upon NMII-A knockdown. In addition, GnT-V mRNA expression was upregulated and GnT-III was downregulated in two NSCLC cell lines and the NMII-A knockdown cells. When C2GnT-M was additionally knocked down via siRNA in NMII-A knockdown cells, the changes in GnT-V and GnT-III expression were reversed. The authors investigated the role of C2GnT-M in EMT, as NMII-A appeared to regulate the EMT. C2GnT-M knockdown in NMII-A knockdown cells reversed NMII-A

knockdown-associated downregulation of E-cadherin and upregulation of vimentin. Knockdown of C2GnT-M alone did not induce a mesenchymal cell morphology; nor did knockdown of NMII-A and C2GnT-M together. In wound healing and transwell assays, knockdown of C2GnT-M in NMII-A knockdown cells deceased cell migration, while inhibition of C2GnT-M alone had no significant effect. C2GnT-M alone did not have an effect on cell motility and morphology. In summary, NMII-A negatively regulates EMT and metastasis via up regulation of C2GnT-M, GnT-V and downregulation of GnT-III.

Mo et al. induced EMT in a human hepatocellular cancer (HCC) or liver cancer cell line (MHCC97-L) with TGF-β1 and found that Smad and Erk1/2 signaling regulated N-acetylglucosaminyltransferase III (GnT-III) expression (Mo et al., 2017.) GnT-III, encoded by *MGAT3*, is a glycosyltransferase that catalyzes the synthesis of bisecting GlcNAc structures; GnT-III has been characterized as a suppressor of tumor metastasis. After treating cells with TGF-β1, the authors confirmed the occurrence of EMT in MHCC97-L cells by their observation of spindle-like cellular morphology and decreased expression of E-cadherin and increased expression of genes encoding N-cadherin and α-SMA at the mRNA and protein levels. The authors previously found decreased GnT-III mRNA expression when they induced EMT with hepatocyte growth factor (HGF) in a different human HCC cell line Huh7. In this study, the authors found decreased GnT-III expression at both the mRNA and protein level in their EMT-induced cell line, as well as a reduction in bisecting GlcNAc structure by fluorescence cell PHA-E lectin-immunochemistry. The authors also investigated the Smad-dependent and Erk signaling pathways, as they have been implicated with TGF-β1 signal transduction in EMT. They found slight increased phosphorylation of Smad3 ($< 1.5 \times$) and Erk1/2 ($> 1.5 \times$) after TGF-β1

treatment, while the total protein was not significantly changed. Next, they pharmacologically inhibited Smad3 and Erk1/2; SB431542 abolishes Smad3 phosphorylation, and U0126 decreases Erk1/2 phosphorylation. TGF-β1 decreased E-cadherin protein expression; however treatment with either compound restored E-cadherin protein level to untreated level. In addition, treatment with SB431542 or U0126 restored GnT-III mRNA expression as well as bisecting GlcNAc structures. The authors conclude that GnT-III expression is regulated by Smad3 and Erk signaling pathways in this TGF-β1-induced EMT model of HCC.

Cui et al. demonstrated how β1,6-GlcNAc glycans contribute to the role of CD147 function in HCC metastasis (Cui et al., 2018.) GnT-V, encoded by *MGAT5* and located in the medial Golgi, catalyzes the addition of β1,6-N-GlcNAc to the alpha-linked mannose of biantennary N-linked oligosaccharides present on newly synthesized glycoproteins. The authors found that GnT-V and EMT were correlated in that GnT-V mediated glycosylation, CD147 protein expression, and CD147-β1,6-branching were elevated during TGF-β1-induced EMT in a normal human hepatic cell line. CD147, also known as basigin, is a tumor-associated transmembrane glycoprotein that carries 1,6-N-acetylglucosamine (1,6-GlcNAc) glycans and in HCC, CD147 is closely associated with EMT, tumorigenesis, and chemoresistance. Next, the authors surveyed the significance of CD147/basigin-β1,6-branched glycans in HCC patients. They analyzed lectin histochemistry of 14 HCC patient samples and observed high levels of CD147/basigin and β1,6-GlcNAc-branched N-glycans. Analysis of 51 patients with HCC revealed that the level of CD147/basigin-β1,6-branched glycans increased with the Barcelona clinic liver cancer (BCLC) stage: patients with stage C disease were markedly positive for CD147/basigin-β1,6-branched glycans, while patients with stage 0-A disease exhibited weak

signals. The authors then studied the effect of GnT-V-mediated glycosylation of CD147/basigin on the invasiveness of HCC cells. They inhibited β1,6-branching synthesis with swainsonine in one HCC cell line and found reduced cell invasion in vitro. In addition, they found reduced MMP-1, MMP-2, and MMP-9 mRNA expression when they treated two HCC cell lines with mutant CD147/basigin with defective β1,6-branched N-glycosylation. The authors next assessed the effect of N-glycosylation on the interaction between CD147/basigin and integrin β1. CD147/basigin interacts with integrin β1 to modulate integrin-dependent signaling and focal adhesion kinase (FAK) activation. This interaction activates the Rac/Ras/Raf/ERK and PI3K/Akt pathways and results in enhanced invasive and metastatic potential of HCC cells. Experiments suggested that binding of CD147/basigin to integrin β1 is affected by N-glycosylation. With swainsonine treatment, the ability of CD147/basigin to bind integrin β1 was decreased. Next, the authors showed that pharmacologic inhibition of PI3K in two HCC cell lines resulted in decreased expression of Gnt-V at both the RNA and protein level. Swainsonine treatment impaired PI3K pathway activation and the subsequent activation of p-FAK, p-paxillin, and p-Akt. In summary, the authors found that β1,6-branching promotes cancer cell invasion and CD147-integrin β1 binding in HCC.

In a more descriptive study, Li et al. also induced EMT in a HCC cell line with hepatocyte growth factor (HGF,) and analyzed changes in cell surface protein glycosylation with lectin microarray and qRT-PCR (Li et al., 2013.) Glycans containing GlcNAc were reduced, and glycans containing β1,6-GlcNAc branching structures were increased. HGF treated cells also had increased invasive potential in transwell migration-invasion assays.

Based on the observation that BGC823 gastric cancer cells had higher levels of GnT-V expression than normal gastric mucosal cells, Huang et al. studied the role of GnT-V in metastatic cellular behavior (Huang et al., 2013.) Knockdown of GnT-V with siRNA resulted in decreased N-linked β1,6-branched glycan levels in BGC823 cells. Proliferation rates were decreased with GnT-V knockdown and cells were sensitized to chemical induction of apoptosis. Cells with decreased GnT-V expression showed impaired migration and invasiveness. Both mRNA and protein expression of EGFR, ErbB2, and ErbB4 were decreased by GnT-V knockdown and E-cadherin expression was increased while vimentin and MMP-9 expression were decreased. Overall, knockdown of GnT-V in these cells led to impaired metastatic behavior and a concurrent shift in molecular phenotype toward epithelial and away from mesenchymal characteristics or an MET.

Pinho and colleagues studied the expression of *Mgat3*, the gene encoding GnT-III, and found a correlation between GnT-III and N-linked glycosylation during EP (Pinho et al., 2012.) In a normal mouse mammary cell system, induction of EMT with TGF-β1 was associated with decreased mRNA expression of *Mgat3* and significant changes in CpG island methylation patterns within the *Mgat1* gene. Induction of EMT was then found to significantly decrease levels of bisecting GlcNAc structures at the plasma membrane. Bisecting GlcNAc structures were found to co-localize with E-cadherin in cells with an epithelial phenotype and this co-localization was abrogated by EMT. Immunoprecipitation experiments showed that the epithelial phenotype was associated with E-cadherin modified by bisecting GlcNAc structures, this glycosylation is decreased by EMT, and E-cadherin glycosylation is rescued by MET. Taken together these data suggest that E-cadherin N-glycosylation with

bisecting GlcNAc structures is regulated during EP or EMT-MET cycling and associated with GnT-III activity.

A global analysis of N-linked glycan presentation and expression in normal mouse mammary epithelial cells undergoing EMT induced by TGF-β was reported by .) Cleavage of N-linked glycans from glycoproteins using PNGase-F was followed by mass spectrometry analysis. As compared to control group cells, those treated with TGF-β displayed a similar number of distinct glycans, but approximately 25% of glycans identified were specific to either control or treated cells, suggesting significant alteration of glycan presentation upon EMT. TGF-β-treated cells expressed more high-mannose N-glycans and fewer complex N-glycans. Treatment with TGF-β resulted in decreased expression of six out of seven N-glycan-related genes, with only *MGAT4B*, the gene encoding GnT-IVb, upregulated. While GnT-IVb catalyzes addition of GlcNAc to complex branching N-glycan structures, the overall decrease in complex N-glycans observed upon TGF-β treatment is thought to result from a significantly greater downregulation of GnT-III as compared to GnT-IV. These findings support a global decrease in N-linked glycans with changes in specific glycan presentation during EMT.

Subsequent work by Tan et al. has implicated loss of GnT-III activity and aberrant glycosylation in promotion of hypoxia-induced EMT in breast cancer cells (Tan, Wang, Li, & Guan, 2018.) Exposure of MCF7 and MDA-MB-231 breast cancer cells to hypoxia induced loss of E-cadherin, increased fibronectin, and elevation of glucose transporter-1 (GLUT1,) thought to be a marker of hypoxia. Hypoxic cells were more elongated and displayed greater capacity for migration. Mass spectrometry analysis of normoxic and hypoxic cell N-glycans found that most

N-glycans specific to hypoxic cells were complex rather than high-mannose. Specifically, bisecting GlcNAc structures decreased with hypoxia, mirroring their earlier findings in TGF-β-induced EMT. Overexpression of GnT-III, responsible for addition of branching GlcNAc moieties to N-linked glycans, inhibited proliferation and migratory capacity in normoxic MCF-7 cells and rescued the hypoxia-inducible E-cadherin downregulation and increased AKT signaling seen in cells with normal GnT-III expression; conversely, knockdown of GnT-III with shRNA enhanced the effects of hypoxia-induced EMT.

Xu and colleagues studied the impact of epidermal growth factor (EGF) on EMT and glycosylation in GE11 epithelial cells (Xu et al., 2017.) Treatment with EGF resulted in elongation, decreased intercellular contact, and increased cell migratory ability consistent with EMT. Levels of E-cadherin were decreased and levels of N-cadherin increased, also suggesting EMT induction by EGF. Lectin-binding studied identified significant decreases in bisecting GlcNAc structures and increases in branching GlcNAc structures after EGF treatment. Overexpression of GnT-III in these cells led to resistance to EGF-induced EMT as measured by relative expression of E-cadherin and fibronectin.

A follow-up study by Xu et al. described the glycosylation changes seen in conjunction with changes in cultured cell density (Xu et al., 2017.) Plating MCF10A human breast cancer cells at progressively lower densities indicated that sparsely plated cells were more elongated than their more densely plated counterparts. This elongated morphology was accompanied by decreased E-cadherin expression, increased N-cadherin and vimentin, and decreased p120-, α-catenin, and γ-catenin. Taken together the low-density phenotype resembles that seen during

EMT. Consistent with this group's reports in an EGF-induced EMT model, low-density cells expressed significantly lower levels of GnT-III and increased GnT-V. Presence of the corresponding glycan structures, bisecting and branched GlcNAc moieties, respectively, was similarly altered. Analysis of β1-integrin N-glycosylation mirrored the overall glycosylation pattern of the cells, with sparsely plated cells displaying higher levels of branched and lower levels of bisecting GlcNAc modifications on β1-integrin.

Hassani et al. found that inhibition of GnT-V, encoded by *MGAT5*, enzymatic activity with the small-molecule inhibitor 3-hydroxy-4,5-bis-benzyloxy-6-benzy-loxymethyl-2-phenyl2-oxo-2l5-[1,2]oxaphosphinane (PST3.1a) restrained glioblastoma multiforme (GBM) growth by affecting microtubule and microfilament integrity of GBM stem cells (Hassani et al., 2017.) Overexpression of *MGAT5* is correlated with cell migration, invasion, and EMT; gliomas express highly variable levels of *MGAT5* mRNA, and GnT-V enzymatic activity changes through the course of gliomagenesis. Glycomimetic compounds, phosphinosugars also called phostines, can possibly interfere with glycosylation in cancer cells and the authors selected the lead compound PST3.1a (3-hydroxy-4,5-bis-benzyloxy-6-benzyloxy- methyl-2-phenyl2-oxo-2l5-[1,2]oxaphosphinane) for further anti-tumor studies. PST3.1a inhibited GnT-V enzymatic activity, but displayed no inhibitor effect against GnT-III enzymatic activity. Next, they studied the glycome of GBM cancer stem cells in vitro grown in the presence or absence of PST3.1a, and confirmed that PST3.1a inhibited GnT-V resulting in decreased multi-branched b1,6-GlcNAc mannose intermediate N-glycans. Knocked down *MGAT5* via siRNA was similar to PST3.1a resulting in lower binding of PHA-L lectin. Additional treatment with PST3.1a further reduced residual binding and reduced the ability of GBM cancer stem cells to form large

25

neurospheres (NS) in two GBM cancer stem cell lines in nonadherent/proliferative conditions. The *in vivo* pharmacologic activity of PST3.1a was then evaluated in orthotropic graft models of GBM using Gli4 and GliT cell lines where they found that PST3.1a treatment significantly reduced the overall Gli4-invaded surface as well as tumor cell densities within invaded areas. Mice treated with PST3.1a survived significantly longer than those treated with vehicle, with a median survival of 108 days versus 79 days for the vehicle cohort. In addition, mice treated with both PST3.1a and temozolomide exhibited a significant survival advantage over those treated with temozolomide alone, with a median survival of 135 days versus 102 days for the vehicle cohort. Finally, using CellMiner and DAVID with the NCI-60 cancer cell line panel, the authors performed transcriptomic analysis and found that mitochondrial gene expression was negatively correlated with PST3.1a cytotoxicity, whereas the expression of genes involved in EMT was positively correlated with the response. In conclusion, PST3.1a inhibits GnT-V, though the anti-tumor effect depends on a cancer cell's EP and energetic metabolic status.

1.6.2 Epithelial plasticity and O-linked glycosylations in cancer

Ye et al. elucidated a novel mechanism linking mucin-type core 3 O-glycan to the EMT-MET plasticity of colorectal cancer (CRC) cells via a MUC1/p53/miR-200c-dependent signaling cascade (Ye et al., 2017.) Mucin-type core 3 O-glycan is one of eight major groups of mucin-type O-glycans; it is synthesized by the enzyme β1,3-N-acetylglucosaminyltransferase-6 (β3gnT6, core 3 synthase,) which is primarily expressed in the human stomach, colon and small intestine. Mucin-type core 3 O-glycan had been implicated in cancer metastasis, but the exact mechanism was unclear. The authors first analyzed mRNA expression levels of core 3 synthase in 497 CRC samples in The Cancer Genome Atlas (TCGA.) Low expression

correlated with lymph node metastasis, distant metastasis, and a poor overall survival for CRC patients. The authors determined that expression levels of core 1 β1,3-galactosyltransferase (C1GalT1); the endoplasmic reticulum chaperone Cosmc involved in C1GalT1 folding; C2GnT1, C2GnT2 and C2GnT3 (three isoforms of core 2 β1,6-N-acetylglucosaminyltransferase (C2GnT)); and core 3 synthase in four human colonic adenocarcinoma cell lines. Low core 3 synthase expression was observed in two of the cell lines (HT-29 and LS174T cells.) Core 3 synthase was transfected to re-express core 3 synthase in these cancer cell lines and these β3gnT6/HT-29 and β3gnT6/LS174T recombinant cells exhibited reduced proliferation, migration, and invasion in vitro compared to mock-transfected cells. Next, the authors found that re-expression of core 3 synthase induced a MET as β3gnT6/HT-29 and β3gnT6/LS174T cells were characterized by increased mRNA and protein levels of E-cadherin and decreased mRNA and protein levels of N-cadherin, snail, slug, ZEB1 and ZEB2. Re-expression of core 3 synthase also led to an increase in terminal GlcNAc residues, which were present on mucin-type core 3 O-glycan in β3gnT6 transfected cells; core 3 synthase targeted protein(s) with high-molecular-weight (> 250 kDa) and not low-molecular-weight proteins (< 250 kDa.) In β3gnT6/HT-29 and β3gnT6/LS174T cells core 3 synthase suppressed the translocation of MUC1-C into the nucleus and led to an increase in MUC1-C in the plasma membrane fraction, as revealed by cell fractionation assay. The final mechanism for MET induction by re-expression of core 3 synthase was found to involve a MUC1/p53/miR-200c axis. Inhibition of MUC1 via siRNA, p53 via siRNA, or miR-200c via an inhibitor in β3gnT6/HT-29 and β3gnT6/LS174T cells resulted in increased expression of E-cadherin and decreased expression of N-cadherin, ZEB1 and ZEB2 expression. Using migration and invasion assays, MUC1 knockdown resulted in reduction in migration and invasiveness, while p53 knockdown or miR-200c inhibitor led to an increase in

migration and invasiveness. The authors found a positive correlation between core 3 synthase, p53 and miR-200c mRNA levels in 52 CRC samples. Finally, *in vivo* athymic mice xenograft tumor growth experiments showed the volume and mass of tumors arising from β3gnT6/HT-29 and β3gnT6/LS174T cells were significantly less than those using mock-transfected cells. In summary, the authors concluded that mucin-type core 3 O-glycan is synthesized in the membrane tethered to MUC1 N-terminal domain, which inhibited MUC1-C nucleus translocation, de-repressing p53 gene transcription and finally activating miR-200c expression that lead to a MET.

Based on the totality of these N- and O-linked glycosylation studies only a few consistent associations have been made with regard to the EP programs of EMT and MET. In normal breast epithelial cells and breast cancer GnT-III activity, responsible for addition of branching GlcNAc moieties to N-linked glycans, seems to be negatively associated with an EMT. Apart from this observation, the field is too nascent for any other reliable comments and would generally suggest a very context dependent association between EMT-MET programs and specific glycosylations that calls for further intensive study.

1.7. Associations between EMT and O-GlcNAcylation

As stated previously, a specific type of O-linked glycosylation, O-GlcNAcylation, is an important posttranslational protein modification regulating diverse cellular processes, such as gene expression, protein stability and cell signaling dynamics. This important biochemical process which is most akin to phosphorylation is controlled by only two highly conserved enzymes: O-linked N-acetylglucosamine transferase (OGT,) which transfers N-acetylglucosamine from uridine diphosphate N-acetylglucosamine (UDP-GlcNAc) to protein

substrates, and N-acetyl-β-glucosaminidase (OGA, O-GlcNAcase,) which removes the O-GlcNAc modification. O-GlcNAcylation regulates practically every cellular process, and plays a major role in the etiology of diseases (Hart, 2014.) However, only recently have we begun to appreciate the important roles of O-GlcNAcylation in EMT promoted malignant transformation and tumor progression.

Hints at the connections between O-GlcNAcylation and EMT related phenotypes include a study by Alisson-Silva and colleagues who examined the relationships between the HBP, EMT, and the O-GalNAcylation of human oncofetal fibronectin (onfFN,) a mesenchymal extracellular matrix glycoprotein implicated in tumor cell invasiveness and proliferation (Alisson-Silva et al., 2013.) They noted that A549 human epithelial lung carcinoma cells exposed to hyperglycemic media displayed increased TGF-β secretion, increased expression of vimentin and N-cadherin, increased motility, and morphological changes consistent with EMT. Hyperglycemia increased expression of UDP-GalNAc:polypeptide N-acetylgalactosaminyltransferase 6 (ppGalNAc-T6,) the enzyme responsible for glycosylation of fibronectin (FN) to form onfFN, and this effect was enhanced by but incompletely dependent on TGF-β signaling. Overexpression of GFAT in A549 cells increased expression of the FN IIICS domain which accepts GalNAc from ppGalNAc-T6, as well as total levels of FN, onfFN, N-cadherin, and vimentin. Taken together these data suggest that the routing of glucose through the HBP plays an important role in the initiation of EMT.

This was corroborated by Jang et al. who recently discovered differential O-GlcNAcylation in colorectal carcinoma (CRC) when analyzing primary CRC and nodal

metastases (Jang, 2016.) Immunohistochemistry was performed on patient tumor samples distinguished as arising from non-neoplastic tissue, centrally within the primary tumor, the invasive front of the primary, or a nodal metastasis. The invasive front was typified by decreased E-cadherin, increased nuclear β-catenin and Snail, and increased O-GlcNAcylation. Central tumor tissue showed intermediate E-cadherin expression, increased O-GlcNAcylation, and levels of nuclear β-catenin and Snail higher than non-neoplastic tissue but lower than the invasive front or nodal metastases. Nodal metastases expressed E-cadherin at levels similar to the tumor center, nuclear β-catenin and Snail similar to the invasive front, and had O-GlcNAcylation levels similar to non-neoplastic tissue. These data suggested a connection between O-GlcNAcylation, invasive behavior, and EMT in human colorectal cancer.

Perhaps these more descriptive data should not have been surprising, as one of the key regulators of EMT–SNAI1 (or Snail or Snail1) was found to be a target of O-GlcNAcylation almost a decade ago. Park and colleagues investigated the stability of the EMT-associated transcription factor Snail1 in the setting of altered O-GlcNAcylation (Park et al., 2010.) Serine 112 is a critical regulatory site on Snail1, with phosphorylation at Ser112 resulting in increased degradation. Immunoprecipitation of Snail1 using an O-GlcNAc-specific antibody was followed by mass spectrometry analysis and site-specific mutation experiments allowed localization of Ser112 as a site of O-GlcNAcylation. Chemical inhibition of O-GlcNAcase, resulting in increased O-GlcNAcylation, led to increased Snail1 protein levels at steady state without impacting mRNA expression of Snail1, as well as decreased ubiquitination of Snail1. Overexpression of UDP-GlcNAc–peptide N-acetylglucosaminyltransferase (OGT,) the enzyme responsible for O-GlcNAcylation of Snail1, led to decreased Ser112 phosphorylation and

increased protein levels of Snail1. Culturing cells in hyperglycemic media increased O-

GlcNAcylation and Snail1 protein levels without increasing Snail1 mRNA expression.

Hyperglycemia did not, however, increase levels of S112A mutant Snail1 which cannot be O-

GlcNAcylated at residue 112. Upregulation of O-GlcNAcylation, both by hyperglycemia and O-

GlcNAcase inhibition, was also found to suppress E-cadherin mRNA transcription, while OGT

inhibition led to increased transcription of E-cadherin mRNA. Finally, overexpression of OGT in

MCF-7 cells increased cellular migration and invasiveness and was largely rescued with

knockdown of Snail1. These findings suggest that O-GlcNAcylation of Snail1, upregulated by

increased influx of glucose through the HBP, increases Snail1 stability and induces an EMT.

A more recent study has since confirmed these O-GlcNAcylation results with Snail1. Gao

et al. carried out mass spectrometry-based proteomic analysis of proteins that interacted with

OGT in HeLa cells and constructed a protein-protein interaction (PPI) network for OGT (Gao et

al., 2018.) Using co-IP, they confirmed from their mass spectrometry data that OGT physically

interacted with the NuRD complex, HDAC1 and HDAC2, which are epigenetic regulators. They

hypothesized that one or more components of the NuRD complex may be substrates of O-

GlcNAcylation, or that OGT may coordinate with the NuRD complex to participate in histone

modification and chromatin remodeling. The authors then focused on elucidating downstream

target genes of OGT; they performed RNA-seq on OGT knockdown and control HeLa cells, and

identified Snail1 and ING4 as important OGT target genes. Snail1 as mentioned is a canonical

EMT-TF, and ING4 is a tumor suppressor that has previously been correlated with high-grade

tumors and poor prognosis. The authors also demonstrated that OGT promoted carcinogenesis

and metastasis in cervical cancer as genetic knockdown of OGT in two cervical cancer cell lines

resulted in delayed cellular migration in an in vitro wound healing assay and a decrease in invasive potential in transwell assay. OGT overexpression in the same cell lines resulted in an increase in invasive potential. Through the Oncomine database, they found that OGT expression was upregulated in cervical cancer compared with adjacent normal tissues. Kaplan–Meier survival analysis of OGT showed that lower expression of OGT was associated with improved survival in cancer patients, when the influence of systemic treatment, endocrine therapy and chemotherapy was excluded. In summary, the authors revealed multiple novel physiological connections between EMT and O-GlcNAcylation using genomic and proteomic analysis.

Harosh-Davidovich et al. have subsequently found that O-GlcNAcylation may enhance cell migration through the regulation of β-catenin and E-cadherin levels in colorectal cancer (CRC) (Harosh-Davidovich & Khalaila, 2018.) The Wnt/β-catenin signaling pathway and cadherin-mediated adhesion are implicated in EMT: β-catenin-mediated transcription upregulates Snail2, which then represses *CDH1* transcription the gene that encodes for E-cadherin. The authors found that with Thiamet-G (TMG,) a potent inhibitor of OGA, murine fibroblast cells demonstrated increased O-GlcNAcylation level as well as increased protein levels of β-catenin and E-cadherin. Silencing OGT in the same fibroblast cell line resulted in decreased protein levels of β-catenin. Using WGA affinity purification, they found that β-catenin is O-GlcNAcylated at four sites in fibroblast cells, and TMG treatment resulted in increased β-catenin transcriptional activity. The authors hypothesized that O-GlcNAcylation may prevent the assembly of β-catenin-APC destruction complex, and thus nuclear translocation of β-catenin is enhanced. Fibroblasts treated with TMG exhibited enhanced migration in a wound closure assay. In addition, in an orthotropic murine model of colorectal cancer, shOGT injected mice exhibited

lower tumor diameter, lower number of metastasis in the mesentery, and a lower mortality rate. shOGA injected mice displayed an enhanced mortality, while shOGT injected mice had a diminished mortality rate. In summary, increased O-GlcNAcylation enhanced cell migration in vitro, and inhibiting O-GlcNAcylation had anti-tumor effects and reduced metastasis in CRC *in vivo.*

1.8 The EMT-HBP-O-GlcNAcylation axis: An important new pathway to the neoplastic phenotype

Very recently, a number of studies have shown that EP may not only be impacted by HBP and subsequent O-GlcNAcylation, but that EMT may actually induce HBP-O-GlcNAcylation for malignant transformation and tumor progression constituting an EP-HBP-O-GlcNAcylation axis. Similar to the other glycosylation described above, there appears to be complex regulation of this axis depending on the cellular context in both feed-forward and feed-back modes.

The association of EMT with upregulated HBP genes in cancer has recently been reported in the stromal cells of the lung tumor microenvironment. Zhang et al. performed an integrated analysis of the transcriptome of human primary non-small cell lung cancers along with [18]fluoro-2-deoxy-D-glucose PET (FDG-PET) scans and identified *GFPT2* of the HBP pathway to be a critical regulator of metabolic reprogramming in the tumor stroma of lung adenocarcinomas (Zhang et al., 2018.) The authors assembled a radiogenomics (RG) study cohort of 130 patients with NSCLC, in which they related clinical glucose uptake via FDG-PET scan to bulk and flow-cell sorted tumor gene expression. The two major histological subtypes, adenocarcinoma and squamous cell carcinoma (SCC,) exhibited differences in glucose uptake

33

and gene expression. Genes more highly expressed in adenocarcinoma were enriched for processes related to extracellular matrix (ECM) remodeling and EMT; genes more highly expressed in SCC were enriched for cell growth and proliferation processes. In regard to glucose metabolism, SCC had higher DEGs in glycolysis and pentose phosphate pathway (PPP,) supporting the utilization of the Warburg effect, whereas adenocarcinomas showed more DEGs in the HBP, suggesting a role extending beyond the Warburg effect. Using cell-type-specific transcriptomics of the NSCLC tumor microenvironment, the authors found a stronger association of altered glucose uptake in the tumor stroma of adenocarcinoma compared with that of SCC. The authors concluded that metabolic reprogramming as well as the molecular pathways and cell types associated with glucose uptake is histology-specific.

In lung adenocarcinoma, they found that *GFPT2* was the only prognostically significant gene correlated to glucose uptake and that it was predominantly expressed in the tumor stroma. As mentioned above, GFPT2 is a rate-limiting enzyme of the HBP pathway which is also upregulated by the EMT. To validate the role of GFPT2 in EMT, the authors induced EMT in NSCLC adenocarcinoma cells with TGF-β and found increased protein levels of GFPT2 coinciding with decreased E-cadherin and increased vimentin protein levels. Next, the authors induced EMT with TGF-β in normal fibroblasts (NF) derived from normal human lung tissue, and found that these NF transformed into cancer associated fibroblasts (CAFs.) In addition, these CAF-like cells expressed HBP genes and EMT genes associated with glucose uptake more highly than NF. At the same time, there was minimal to no change in genes related to glycolysis, PPP, and TCA cycle in these cells. Next, the authors also treated NSCLC adenocarcinoma cell lines (A549, HCC827, and NCI-H358) with TGF-β and found that glucose metabolism genes

associated with energy production and cell proliferation (glycolysis, PPP, and the TCA cycle) were mostly unchanged, whereas most EMT genes and several HBP genes correlated directly with increased glucose uptake. In summary, the authors conclude that metabolic reprogramming glucose uptake in tumor stroma correlated strongly with EMT and the HBP.

More direct experimental data linking EMT to the induction of the HBP and increased O-GlcNAcylation come from Lucena et al. who described effects of TGF-β-stimulated EMT in A549 NSCLC cells (Lucena et al., 2016.) Treatment of these cells with TGF-β resulted in increased uptake of the fluorescent glucose analogue 2-(N-(7-nitrobenz-2-oxa-1,3-diazol-4-yl)amino)-2-deoxyglucose without changes in lactate, ATP, pyruvate, or glycogen content. Proteomic analysis identified increased protein expression of several enzymes involved in synthesis of the oligosaccharide precursor necessary for protein glycosylation within the ER. Additionally, GFAT1 expression and UDP-GlcNAc production were increased after stimulation of EMT with TGF-β, while glycolytic enzymes downstream of hexokinase as well as pentose phosphate pathway enzymes were stable or downregulated, demonstrating shunting of glucose through the HBP. Characterization of glycoproteins in A549 cells undergoing EMT showed increased glycans with terminal α2-6Neu5Ac groups, poly-N-acetyl-lactosamine, and α-fucose, as well as increased high-mannose N-glycans. Glycans terminating in β-Gal were decreased. Not surprisingly, this glycophenotype differs from that reported in equine EMTCs (Lange-Consiglio et al., 2014,) underlining the complexity and specificity of protein glycosylation. Overall, levels of O-linked GlcNAc were increased, as was expression of the enzyme responsible for this modification, OGT. Finally, in the absence of TGF-β stimulation, induction of O-GlcNAcylation was sufficient to induce morphologic, molecular, and behavioral changes consistent with EMT,

suggesting that O-GlcNAcylation is an instigating factor in EMT rather than a consequence thereof.

In addition to the links established between EMT-HBP-O-GlcNAcylation *in vitro* in this one cell line by Lucena et al., Taparra et al. demonstrated that the EMT-HBP axis was capable of accelerating *Kras* mutant lung tumorigenesis, and could be targeted genetically and pharmacologically to produce anti-tumor effects (Taparra et al., 2018.) Using genetically engineered mouse models of $Kras^{G12D}$-induced lung tumors, co-overexpression of EMT-TFs *Twist1* or *SNAIL1* was capable of accelerating lung tumorigenesis by inhibition of the tumor suppressor barrier known as oncogene-induced senescence (OIS) (Taparra et al., 2018; Tran et al., 2012.) To identify differentially expressed genes (DEGs) in lung tumors derived from these mouse models expressing $Kras^{G12D}$ alone, $Kras^{G12D}$/*Twist1*, and $Kras^{G12D}$/*Snail1*, mRNA microarray analysis was performed and revealed genes involved in "metabolic biological processes." Mouse lung tumors overexpressing *Twist1* or *SNAIL1* exhibited increased expression of critical genes in the HBP pathway, specifically *GFPT2* and *UAP1*. Verifying this EMT-HBP axis, overexpression of *SNAIL1* or *Twist1* in human mutant *KRAS*-driven NSCLC cell lines resulted in similar overexpression of HBP genes. Genetic and pharmacologic inhibition of the HBP pathway resulted in cellular senescence in human normal lung cells and NSCLC cells. This premature senescent phenotype was rescued with the bypass GlcN metabolite in normal human lung cells. In addition, in both mouse xenograft and autochthonous lung tumor models, pharmacological inhibition of HBP with DON therapeutically reduced the size of established tumors and inhibited early lung tumorigenesis, respectively, through the induction of senescence and/or cell death. Reversed phase HPLC analysis of human NSCLC cell lines showed that

Twist1 overexpression resulted in increased HBP flux via increased levels of UDP-HexNAc (UDP-GlcNAc and downstream metabolite UDP-GalNAc.) In addition, OGT protein levels and total O-GlcNAcylation level were increased in both human NSCLC cells and mouse lung tumor tissues that overexpressed EMT-TFs. The HBP pathway was required for $Kras^{G12D}$-induced lung tumorigenesis as OGT deficiency produced by using OGT knockout mice was characterized by a significant delay in lung tumor development. EMT-HBP-O-GlcNAcylation may suppress OIS by stabilizing oncoproteins such as c-Myc which have been shown previously to be O-GlcNAcylated and restrain OIS. Genetic and pharmacological inhibition of O-GlcNAcylation resulted in a reduction of c-Myc protein levels in NSCLC cells *in vitro* and *in vivo*. In summary, the EMT-HBP-O-GlcNAcylation axis suppresses cellular senescence and accelerates *Kras* mutant lung tumorigenesis (Figure 1.3.)
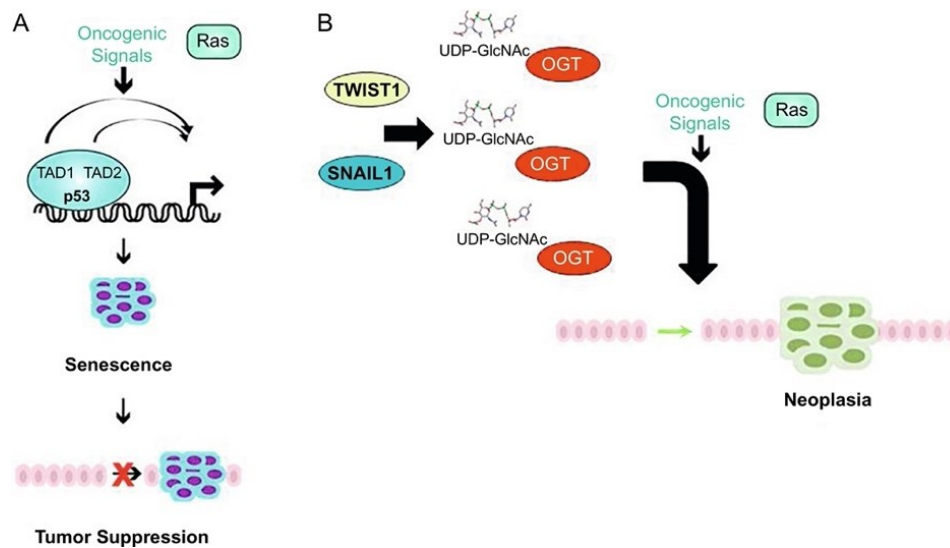

Figure 1.3 Epithelial-mesenchymal transition-transcription factors metabolically reprogram normal epithelial cells toward a neoplastic-prone state.

A) Aberrantly activated mutant RAS protein leads to premature cellular senescence of lung epithelial cells as shown by blue cells that is enforced by p53-dependent oncogene-induced senescence. B) Epithelial-mesenchymal transition-transcription factors (EMT-TFs) TWIST1 and SNAIL1 reprogram epithelial metabolism toward a tumorigenic permissive state by upregulation of the final product of the hexosamine biosynthesis pathway, UDP-N-acetylglucosamine (UDP-GlcNAc,) and the O-GlcNAc transferase (OGT)—the enzyme responsible for adding GlcNAc molecules onto proteins. This metabolic shift leads to increased global O-GlcNAcylation that in the background of activated mutant RAS protein results in increased $Kras^{G12D}$-induced lung tumorigenesis.

Furthermore, Jiang et al. found that O-GlcNAcylation promotes the metastatic potential of colorectal cancer via a miR-101-O-GlcNAc/EZH2 regulatory feedback circuit (Jiang et al., 2019.) TCGA analysis revealed that OGT mRNA level was significantly elevated in all types of CRC, including cecum adenocarcinoma, colon adenocarcinoma, colon mucinous adenocarcinoma, rectal adenocarcinoma, and rectal mucinous adenocarcinoma, compared with that in normal colorectal tissues; there was no significant change in OGA mRNA level in CRC. In addition, in 15 cases of CRC patients with lymph node metastases, the expression of O-GlcNAcylation significantly differed between the tumor and lymph node metastases. Next, the authors examined the expression of OGT, OGA, and O-GlcNAcylation in five human CRC cell lines (LoVo, SW620, SW480, HCT-116, and HT-29) and the normal human intestinal epithelial cell line HCoEpiC. They found that O-GlcNAcylation level was significantly increased in all cancer cell lines compared with that in HCoEpiC cells. Overexpression of OGT or treatment with OGA inhibitors PUGNAc and TMG increased CRC migration and invasiveness via

transwell assays in SW480 cells. In a xenograft murine model using SW480 and SW620 cells, downregulation of O-GlcNAcylation via OGT shRNA in SW620 cells resulted in a significant reduction in the number of metastatic nodules in the liver and lung. When OGT and O-GlcNAcylation were upregulated, the number of metastatic nodules increased.

These authors (Jiang et al., 2019) then implicated the epigenetic factor Enhancer of Zeste Homolog 2 (EZH2) in regulating the EMT in an O-GlcNAcylation-dependent fashion contributing to this increase in metastasis. Downregulation of OGT resulted in decreased expression of mesenchymal markers fibronectin and vimentin, and increased localization of Claudin 7 and E-cadherin on the cell membrane; upregulation of O-GlcNAcylation resulted in the opposite change. Co-IP was performed in SW480 OGT overexpression cells using OGT and O-GlcNAc antibodies, and the co-IP proteins were analyzed by liquid chromatography with tandem mass spectrometry (LC-MS-MS.) Among the ~ 200 proteins observed was histone methyl-transferase EZH2 which is a key epigenetic regulator that catalyzes the tri-methylation of lysine 27 on histone H3 (H3K27me3) and known EMT inducer that participates in the metastasis of various cancers. Treatment with GSK-343, a specific inhibitor of EZH2, inhibited the upregulated invasiveness and reversed the change of EMT markers that was induced by hyper-O-GlcNAcylation. This result was reiterated by genetic knockdown of EZH2 via siRNA.

Next, the authors (Jiang et al., 2019) validated that EZH2 was itself modified by O-GlcNAcylation in SW480 cells. They further tested whether O-GlcNAcylation affected the stability of the EZH2/PRC2 complex. Co-IP experiments showed that the binding capacity of EZH2 and SUZ12, another indispensable component of PRC2, was increased when the O-

GlcNAcylation of EZH2 was upregulated by TMG treatment. In addition, O-GlcNAcylation

enhanced EZH2 protein stability by prolonging the half-life of degradation and suppressing

its ubiquitination. O-GlcNAcylation of EZH2 significantly decreased its ubiquitination level.

Next, the authors showed that miR-101 regulates OGT expression in CRC. Using several web-

based target prediction algorithms (TargetScanS, miRanda, pictar, and PITA) to identify

miRNAs that could potentially target OGT, they identified miR-101 as a potential regulator of

OGT expression. This was confirmed by a luciferase reporter assay, in which the luciferase

activity of the reporter constructs containing OGT 3′-untranslated region (UTR) was most

significantly reduced by a miR-101 mimic construct, as well as a "rescue" experiment using

miR-101 to target a mutated seed sequence of miR-101 at the OGT 3′-UTR. Examining the miR-

101 expression levels in human CRC cell lines, the authors found that miR-101 was significantly

decreased in all cancer cell lines compared with that in the HCoEpiC cell line. When SW620

cells were transfected with the miR-101 mimic, OGT and EZH2 protein levels decreased;

SW480 cells similarly transfected had increased OGT and EZH2 levels. In addition, SW620 cells

transfected with miR-101 mimics had a significant decrease in migratory and invasive abilities;

silencing miR-101 in the SW480 cells with an antisense oligonucleotide inhibitor significantly

increased cell migration and invasion. Next, the authors showed that miR-101 regulates EMT by

targeting OGT and EZH2 such that transfection with miR-101 resulted in decreased protein level

of fibronectin and O-GlcNAcylation levels, as well as increased level of E-cadherin in SW620

cell. The opposite effects were seen in SW480 cells with a miR-101 inhibitor. In addition,

overexpression of OGT or EZH2 in the SW480 cells reversed miR-101-mediated decrease in

fibronectin protein expression and increase of E-cadherin protein expression.

Finally, Jiang et al. (2019) hypothesized that OGT feedback may transcriptionally silence miR-101 in an EZH2-dependent manner. They found that when OGT or EZH2 were downregulated, the levels of mature miR-101, precursor miR-101-1, and precursor miR-101-2 were increased; however if EZH2 was silenced in advance, there was no significant change when OGT was downregulated. Results from ChIP-qPCR analysis of the transcriptional start regions (TSSs) of miR-101-1 and miR-101-2 precursors verified that the miR-101 promoter regions were highly enriched in EZH2, H3K27me3, and O-GlcNAcylation. In addition, EZH2 knockdown in SW480 cells almost completely eliminated the enrichment of O-GlcNAcylation and H3K27me3 in the mIR-101 TSS region. When O-GlcNAcylation was upregulated, the H3K27me3 enrichment in these regions was significantly increased. Meanwhile, the knockdown of EZH2 in SW620 eliminated the enrichment of O-GlcNAcylation in the miR-101 TSS regions, while the knockdown of OGT in the same cell line eliminated the enrichment of H3K27me3 in this region. These results support the hypothesis that O-GlcNAcylation feedback negatively regulates miR-101 and that EZH2 is a necessary component of this loop. In summary, in CRC cells, miR-101/O-GlcNAcylation/EZH2 signaling forms a feedback loop that promotes EMT-mediated metastasis. The downregulation of miR-101 in CRC promotes the elevation of O-GlcNAcylation and thus enhances EZH2 protein stability and function, which, in turn, further reduces the expression of miR-101.

1.9 Conclusions

In summary, EP drives metabolic reprograming and facilitates a number of context-specific, complex glycosylation events. Depending on the context EP programs are associated with intricate changes, both positive and negative in nature, to extracellular and

intracellular glycoconjugates that are associated with the neoplastic phenotype. In this chapter, we also highlight the emerging knowledge of an EP-mediated glycosylation event, the redirection of increased glucose flux toward the HBP resulting in increased global cellular O-GlcNAcylation, which recent data suggest can contribute to tumorigenesis and cancer progression. Although the HBP-O-GlcNAcylation axis is emerging as an important pathway in the cancer cell during EMT, the precise molecular mechanisms of O-GlcNAcylation modification during EMT promoted tumorigenesis and metastasis remain to be elucidated. Further investigations are needed to identify novel O-GlcNAcylated proteins involved in signaling pathways leading to downstream execution of EP programs. It is also likely that the role of EMT-HBP-O-GlcNAcylation discussed here may extend beyond cancer development and metastasis to include other known EMT-related phenotypes such as cancer treatment resistance to radiation, cytotoxic systemic agents, targeted therapies and immunotherapies (Arumugam et al., 2009; Efimova et al., 2016; Shintani et al., 2011; Yochum et al., 2019; Zheng et al., 2015.) In addition, although EP programs are highly conserved developmental programs that have been studied for decades, the requirement of this EMT-HBP-O-GlcNAcylation axis in normal development is unknown and deserves analysis. Finally, the HBP and O-GlcNAcylation present themselves as important potential novel targetable pathways to target EP in cancers.

Note: the preceding introductory section was adapted from: Ryan M. Phillips*, Christine Lam*, Hailun Wang, Phuoc T. Tran. Bittersweet tumor development and progression: Emerging roles of epithelial plasticity glycosylations. *Advances in Cancer Research* 2019. 142:23-62. (*indicates equal contribution)

Chapter 2: Defining the EMT-HBP-O-GlcNAcylation axis as a cancer cell-autonomous mechanism for Twist1-induced metastasis in hepatocellular carcinoma

2.1 Background on *Myc-Twist1* genetically engineered mouse models of metastasis

Hepatocellular carcinoma (HCC) is the most common type of primary liver cancer, representing 90% of all cases (Llovet et al., 2016.) Worldwide, liver cancer is the fourth most common cause of cancer-related deaths (World Health Organization.) HCC is frequently diagnosed at advanced stages, when curative treatments are no longer available and the 5 year-survival rate is only 2% (American Cancer Society.) The majority of HCC occurs in patients with underlying liver disease, such as hepatitis B or C infection, alcohol abuse, and non-alcoholic fatty liver disease. The resulting chronic inflammation or cirrhosis favor a series of genetic and epigenetic changes that culminate in the formation of HCC (Ju et al., 2015.) The MYC oncogene is a major driver of HCC pathogenesis, as it is amplified in about 20% of HCC patients (cBioPortal.) Additional genetic and epigenetic alterations result in metastatic HCC. Overexpression of the epithelial-mesenchymal transition (EMT) transcription factor Twist1 has been shown to correlate with increased HCC invasion and metastasis. Twist1 has been shown to be overexpressed in metastatic human HCC cell lines (Lee et al., 2006.) In addition, Twist1 is overexpressed in HCC patient metastases compared to the primary liver tumor (Lee et al., 2006.)

Unfortunately, the mechanisms by which Twist1 induces metastasis in HCC are poorly understood.

We utilize a suite of novel autochthonous conditional mouse models to study the role of Twist1 in HCC metastasis: LM, LMT, LMF191G, and LMDQD. In collaboration with Dean Felsher at Stanford University, we have an autochthonous conditional model of *MYC*-induced HCC, *LAP-tTA/tetO-MYC* ("LM") (Schachaf et al., 2004.) Upon removal of doxycycline drinking water, LM mice form HCC primary liver tumors. In addition, we have generated a Myc-Twist mouse model, *LAP-tTA /tetO-MYC/Twist1-tet-O-Luc* ("LMT",) that is characterized by metastases to the lung, spleen and lymph nodes (Dhanasekaran et al., 2020) **(Figure 1.1A.)** Expression profiling suggests that LMT primary tumors are highly similar to human HCC tumors associated with *MYC* overexpression and poor prognosis. We have created novel and the first transgenic HCC mouse models with inducible Twist1 mutants, *LAP-tTA/tetO-MYC/Twist1F191G-tet-O-Luc* (LMF191G) and *LAP-tTA/tetO-MYC/Twist1DQD-tet-O-Luc* (LMDQD) **(Figure 1.1B.)** The LMF191G model is characterized by inducible MYC in addition to inducible Twist1F191G which has a loss of function mutation in Twistbox, making it unable to transactivate E-box containing target genes (Massberg et al., 2015.) The LMDQD model is characterized by inducible Myc and inducible Twist1DQD, which is a phosphomimetic in the bHLH domain that confers altered dimerization properties (Gajula et al., 2015.) Functionally, in metastasis-free survival, LMF191G mice are similar to LM mice while LMDQD mice are similar to LMT mice **(Figure 1.1C.)**

In 2020, a non-cancer cell autonomous mechanism for metastasis in the LMT model was reported. It was discovered that MYC and Twist1 cooperate to induce a cytokinome that elicits

recruitment and polarization of tumor associated macrophages to M2 phenotype. Systemic

treatment with Ccl2 and Il13 induced LM tumors to metastasize, while blockade of Ccl2 and Il13

eliminated LMT metastasis. In conclusion, we know that Twist1 promotes metastasis in *MYC*-

induced HCC as well as a non-cancer cell autonomous mechanism for it. The goal of my project

was to define a cancer cell autonomous mechanism of Twist1-induced metastasis in HCC.

2.2 Identification of gene and protein candidates that are implicated in Twist1-mediated metastasis in *MYC*-induced HCC

We conducted multi-omic differential profiling between our LMT, LMT, LMF191G, and

LMDQD models using RNA-seq and quantitative mass-spectrometry based proteomics to

identify candidates that are implicated in Twist1-mediated metastasis in *MYC*-induced HCC. We

were interested in genes that were differentially expressed across four comparisons: 1) Twist

versus non-Twist primary tumors, 2) primary liver tumor versus normal liver, 3) lung metastasis

versus primary liver tumor, and 4) normal lung versus normal liver. Principal component

analysis showed that primary liver tumor, lung metastasis, normal lung, and normal liver are

distinct groups **(Figure 1.2A.)** In addition, these groups clustered together by their expression

profiles **(Figure 1.2B.)** Interestingly, LMT and LM primary liver tumors had similar expression

profiles. From the transcriptomic data, 62 genes were differentially expressed across all four

comparisons and were candidates that correlate with Twist1-induced metastasis in *MYC*-induced

HCC **(Figure 1.2C.)** From the integrated transcriptomic and proteomic data, one gene was

differentially expressed across all four comparisons: *Fgl1* **(Figure 1.2D.)** 91 genes were

differentially expressed across three of the comparisons (primary liver tumor versus normal liver,

lung metastasis versus primary liver tumor, and normal lung versus normal liver) and were candidates that correlate with metastasis.

2.2.1   Olfactory receptors

Interestingly, olfactory receptor pathways were enriched in pathway analysis on the transcriptomic and integrated transcriptomic and proteomic datasets. Several olfactory receptors were overexpressed in lung metastases versus primary liver tumor. Olfactory receptors (OR) are G-coupled protein receptors (GPCRs) and have diverse roles outside of smell (Dalesio et al., 2018.) Ectopic expression of ORs have been found in almost all tissues of the human body (Pluznick et al., 2009; Flegel et al., 2013; Zhang et al., 2007,) and they have been implicated in various cancers, including prostate (Cao et al., 2015; Neuhaus et al., 2009,) liver (Massberg et al., 2015,) and intestine (Braun et al., 2007.) However, they have an unknown role in HCC invasion-metastasis. Of the 66 olfactory receptors that were overexpressed >2-fold in the metastases vs primary tumor, 19 had human orthologs **(Figure 2A**.) Through *in silico* analysis on cBioPortal, OncoMine, and Protein Atlas, *OR6C6, OR9K2, OR2AK2*, and *OR51E2* were determined as candidate olfactory receptors for mechanistic study. *OR2AK2* was overexpressed more than 2-fold in the RNA-seq dataset ($p<0.004$); in addition, it was amplified in 5% of HCC patients and expressed at the protein-level in HCC patients. *OR51E2* was overexpressed 4-fold in the RNA-seq dataset ($p<0.02$); it is genetically modified in 0.7% of HCC patients and overexpressed 4-fold at the RNA-level. Unpublished work by Steven An, formerly at Johns Hopkins University School of Public Health, revealed a role for *OR51E2* in metastasis in non-small cell lung cancer. OR6C6 was overexpressed more than 2-fold in the RNA-seq dataset ($p<0.005$,) genetically modified in 0.4% of HCC patients, and expressed at the protein level in

HCC patients. *OR9K2* was overexpressed over 19-fold in the RNA-seq dataset ($p<0.0004$,) genetically modified in 0.2% of HCC patients, and expressed at the protein level in HCC patients. Kaplan-Meier estimates on cBioPortal showed that none of the OR candidates had a statistically significant effect on disease/progression-free and overall survival. *OR52B2* was added to the list of candidate ORs for mechanistic study. Although it was not identified from the RNA-seq and proteomics data, it looked interesting based on the Kaplan-Meier estimates on cBioPortal. Patients with genetic alterations in *OR52B2* have significantly worse disease-free survival (2.73 months vs 29.66 months, $p=0.000001241$) and overall survival (6.41 months vs 83.18 months, $p=0.0007575$.) Olfactory receptors were transfected into LM and LMT liver tumor-derived organoids, and invasion into collagen was determined after 5 days. OR overexpression was confirmed through immunofluorescent staining **(Figure 2B.)** Olfactory receptors generally increased invasion in HCC organoids, but it was not statistically significant by pair wise analysis **(Figure 2C.)**

2.2.2 Metabolic processes

In both the transcriptomic and integrated transcriptomic and proteomic datasets, metabolic processes were enriched in the GO and KEGG pathway analyses. Around 30% of genes involved in metastasis in the transcriptomic dataset are involved in metabolic processes. The enriched metabolic processes include amino acid metabolism, glycerolipid metabolism, sphingolipid metabolism, and fatty acid biosynthesis **(Figure 3A.)** Similarly, the integrated transcriptomic and proteomic dataset showed an enrichment for metabolic pathways. 21.6% of genes involved in metastasis are involved in metabolic processes. The enriched metabolic processes include amino acid metabolism, ascorbate metabolism, and aldarate metabolism. **(Figure 3B.)**

Of interest, *Gfpt2*, one of the two rate-limiting enzymes in the HBP, was overexpressed more than 2-fold in lung metastases vs primary liver tumor. Clinical datasets on cBioPortal show that HCC patients commonly have genetic alterations in all of the HBP enzymes, and the majority of these alterations are amplifications. In addition, HCC patients have high mRNA expression of the HBP enzymes **(Figure 3C.)** Kaplan-Meier estimates from cBioPortal show that HCC patients with genetic alterations in *GFPT2* and/or its isoform *GFPT1* have significantly worse overall median survival compared to patients without these alterations (27.5 months vs 83.24 months*, p* = 0.006) **(Figure 3D.)**

2.3 HBP-O-GlcNAcylation is sufficient and required for Twist1-induced migration and invasion *in vitro* and *ex vivo*

2.3.1 Cell lines

The effect of HBP modulations on *in vitro* migratory and invasive capabilities were measured in the human HCC lines Huh7, Hep3B, and HepG2 and the murine HCC lines LMT and LM. Treatment with Thiamet-G (TMG) or genetic overexpression of GFPT2 increased global O-GlcNAcylation **(Figure 4A)** as well as migration 2.4-fold (*p*=0.0374) and invasion 3.2-fold (*p*=0.0087) across all cell lines **(Figure 4B.)** Treatment with 6-diazo-5-oxo-L-norleucine (DON) or genetic knockdown of GFPT2 decreased global O-GlcNAcylation **(Figure 4C)** as well as migration 1.8-fold (*p*<0.001) and invasion 2.5-fold (*p*<0.001) across all cell lines **(Figure 4D.)**

2.3.2 Tumor-derived organoids

Organoids derived from LMT and LM primary liver tumors were treated with DON or TMG for 5 days, and invasion and dissemination into collagen were measured. DON treatment reduced global O-GlcNAcylation as well as invasion 2-fold ($p<0.0001$) and dissemination 3-fold ($p<0.0001$) **(Figure 5.1.)** TMG treatment increased global O-GlcNAcylation as well as invasion 2-fold ($p<0.0001$) and dissemination 2-fold ($p=0.0225$) in LMT organoids. Similarly, DON treatment in LM organoids decreased global O-GlcNAcylation and invasion 2-fold ($p<0.0001$) while TMG treatment increased global O-GlcNAcylation and invasion 2-fold ($p<0.0001$) **(Figure 5.2.)**

2.4 Targeting the HBP *in vivo*

DON (20 mg/kg) reduced tumor burden in nude mice subcutaneously injected with LMT cells **(Figure 6A.)** Similarly, when DON treatment was initiated in LMT mice a week after they were taken off doxycycline drinking water, the mice failed to develop liver tumors (data not shown.) Because DON had an anti-tumor effect and I wanted to evaluate the effect of DON on metastasis alone, I used circulating tumor cells and tumor cell colonization in distant organs as an *in vivo* metric for metastasis. We have previously detected circulating tumor cells in the LM and LMT models using a GFP-expressing adenoviral probe that detects elevated telomerase activity in cancer cells **(Figure 6B.)** Treatment with DON (20 mg/kg) was initiated four weeks after LMT mice were taken off doxycycline drinking water. qPCR for *Twist1* mRNA in whole blood showed that DON reduced circulating tumor cells almost 6-fold ($p=0.0304$) **(Figure 6C)** as well as tumor cells >2-fold in the lungs ($p=0.0033$,) and >2 fold in the spleen ($p=0.0033$) **(Figure**

6D.) qPCR for *c-Myc* mRNA revealed a >2-fold reduction in tumor cells in the lungs ($p<0.002$) and >3-fold reduction in the spleen ($p=0.0003$.)

2.5 Pathways that may be regulated by O-GlcNAcylation during HCC invasion-metastasis

2.5.1 c-MYC

c-MYC has been reported to be O-GlcNAcylated at Thr58, which is a known phosphorylation site that leads to c-MYC degradation (Chou et al., 1995.) In addition, it has been shown that OGT levels correlate with c-MYC protein levels but not with c-MYC mRNA levels. Thus increased O-GlcNAcylation may stabilize c-MYC and increase total c-MYC protein levels. C-MYC protein levels are higher in LMT liver tumors compared to LM liver tumors and correlate with increased global O-GlcNAcylation in LMT tumors **(Figure 7A.)** Immunofluorescent staining on invading LMT organoids show that O-GlcNAc and c-MYC overlap at the invasive leading edges **(Figure 7B.)**

2.5.2 PKD

Prkd1 encodes PKD1, or Protein Kinase D1, which is a serine/threonine kinase important for the regulation of cell shape and motility through cytoskeletal remodeling. *Prkd1* has been shown to be a transcriptional target of Twist1 and required for Twist1-mediated dissemination in breast cancer (Georgess et al., 2020.) In the integrated transcriptomic and proteomic dataset, *Prkd1* was expressed 13-fold higher in LMT lung metastases vs the primary liver tumor ($p=1.61\text{x}10\text{-}6$) **(Figure 8A.)** Indeed, in invading LMT organoids, PKD1 levels were significantly higher compared to non-invading LMT organoids **(Figure 8B.)** Treatment with the PKD1 inhibitors

Gö-6976 and kb-NB142 decreased invasion 2 to 3-fold ($p<0.0001$) and dissemination 4 to 6-fold ($p<0.0001$) in LMT organoids **(Figure 8C.)** Interestingly, PKD1 inhibition in LMT organoids significantly decreased global O-GlcNAcylation **(Figure 8D.)**

2.5.3 HA

Hyaluronan (HA) is synthesized from UDP-GlcNAc and UDP-GlcUA by HAS1, HAS2, and HAS3. Glucose supplies the nucleotide sugars needed as building blocks for HA. HAS2 can be O-GlcNAcylated, which significantly increases its activity and stability (Vigetti et al., 2012.) Thus, HA may accumulate due to increased HBP providing building blocks for HA and also HBP O-GlcNAcylation of HAS2. Pathway analysis from the transcriptomic dataset revealed that hyaluronoglucosaminidase activity, HA binding, HA biosynthetic process, and HA metabolic process are specific to lung metastases vs primary tumor, liver tumor vs normal liver, and Twist vs nonTwist **(Figure 9A.)** In addition, *Has1* is expressed >46-fold higher in the lung metastases over the primary liver tumor ($p=0.002$.) HA binding partner *Cd44* is expressed >9-fold higher in the lung compared to the liver ($p<8.13x10\text{-}12$) **(Figure 9B.)** Clinical datasets on cBioPortal reveal that HAS is important in HCC pathology. *HAS1* and *HAS2* are frequently amplified in HCC patients (1.7% *HAS1*, 10% *HAS2*, 0.3% *HAS3*.) Kaplan-Meier estimates show that HCC patients with genetic alterations in *HAS1, HAS2,* and/or *HAS3* have significantly worse overall median survival compared to patients without these alterations (48.95 months vs 83.24 months*, p* = 0.002235) **(Figure 9C.)**

2.6 Characterization of the metastatic tumor subpopulation through single-cell profiling

The bulk RNA-seq dataset showed that LMT and LM liver tumors have similar expression profiles (Figure 1.2A, 1.2B) despite driving different metastatic phenotypes. We sought to profile the metastatic subpopulation in the LMT model through single cell RNA-seq on LM liver tumor and lung, LMT liver tumor and lung, and wildtype liver and lung. Single cells from the livers and lungs of LMT, LM, and wildtype mice were clustered together by their expression profiles and cell labels were assigned to clusters **(Figure 10.1A.)** Interestingly, immune cells were overrepresented in LMT vs LM livers **(Figure 10.1B.)** UMAP clustering and differential expression analyses on LM and LMT liver hepatocytes reveal distinctions between LM and LMT liver hepatocytes **(Figure 10.1C, 10.1D.)** Imputed gene expression showed that LMT liver hepatocytes generally have higher expression amongst genes associated with hexosamine, PKD1, and HA pathways **(Figure 10.2, 10.3, 10.4.)** The Bayesian non-negative matrix factorization method CoGAPS was applied to assess common gene expression patterns across all cell types, as well as cell type specific patterns. CoGAPS patterns that discriminate between LM and LMT liver hepatocytes were identified **(Figure 10.5A.)** Genes in the hexosamine, PKD, and HA pathways show higher weighting for the LMT-associated patterns than the LM-associated patterns **(Figure 10.5B.)**
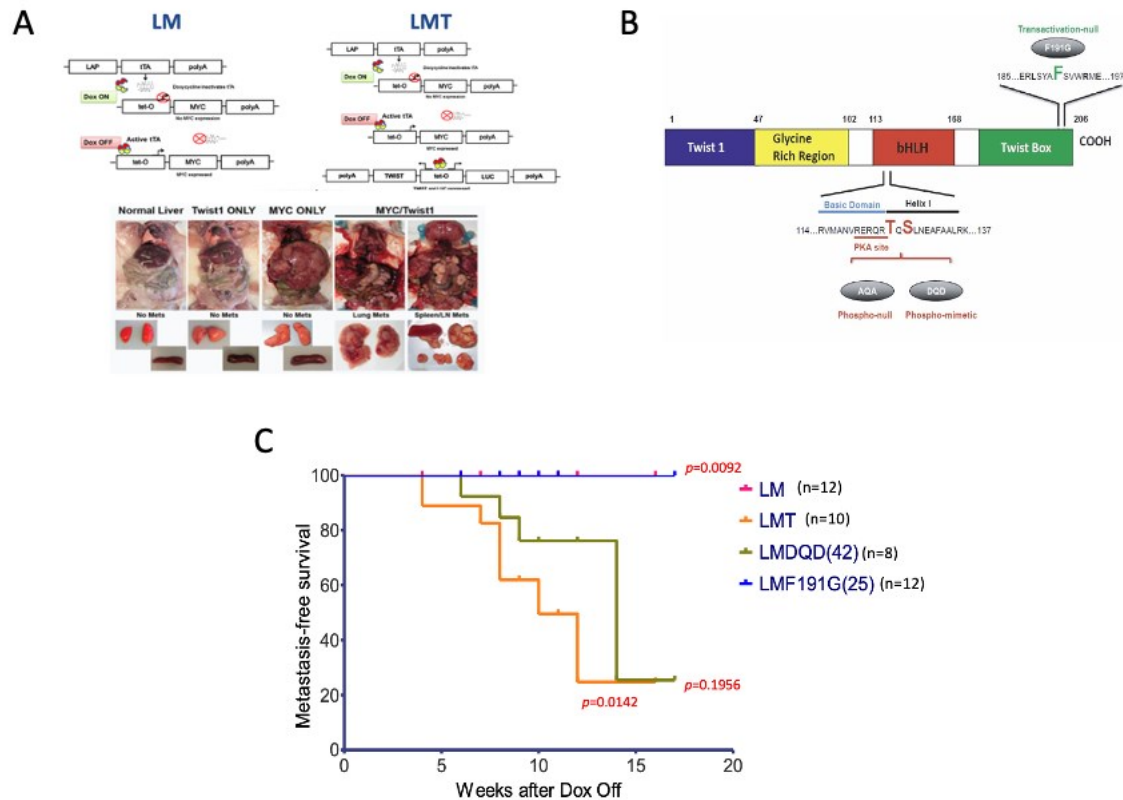
2.7 Figures with legends

Figure 1.1 *In vivo* models of HCC metastasis.

A) Expression of *MYC* and *Twist1* are liver-specific and inducible in the LM and LMT models. *MYC* expression induces the formation of HCC liver tumors. *Twist1* expression promotes metastasis of *MYC*-induced tumors to the lung, spleen, and lymph nodes. B) Structure-function of Twist1. C) LMT and LMDQD have similar metastasis-free survival, while LM and LMF191G are similar.
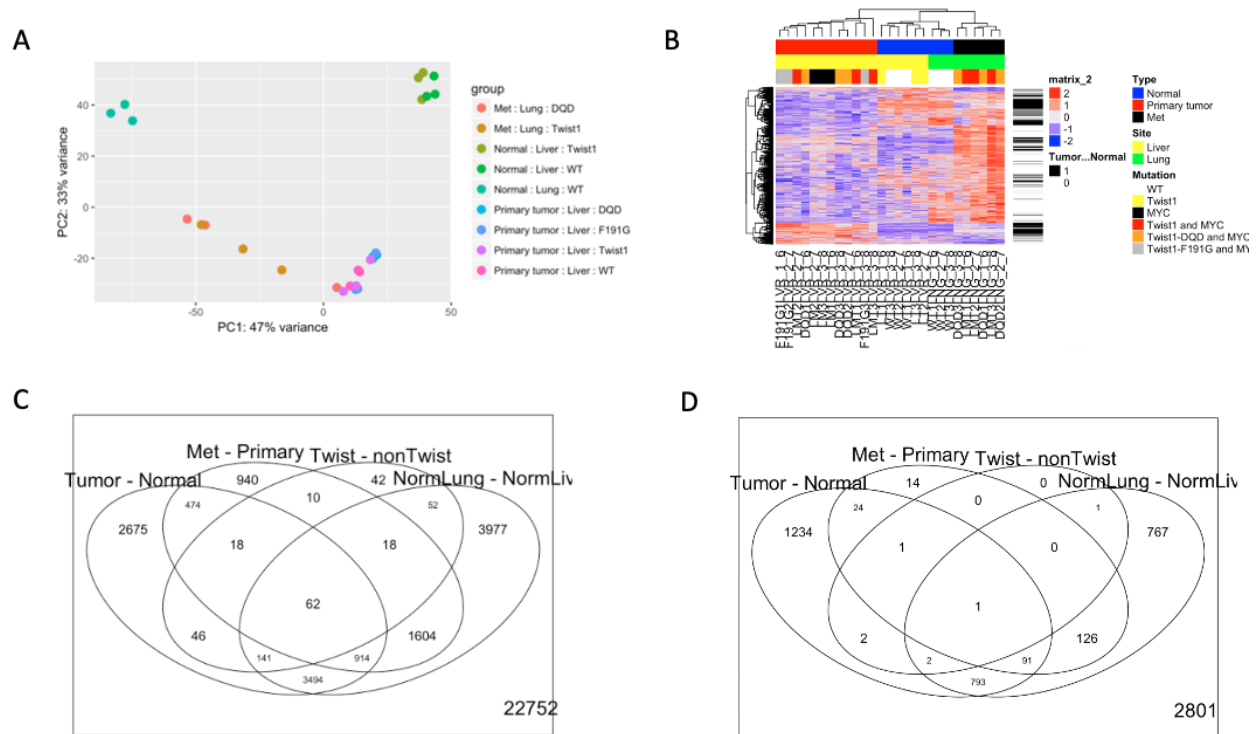
Figure 1.2 RNA-seq and proteomics to identity candidates that correlate with metastasis.

A) Principal component analysis shows that liver tumors, lung metastases, normal liver, and normal lung are distinct groups. B) Expression heatmap reveals that these distinct groups cluster together by their expression profiles. C) Venn diagram of statistically significant genes from tumor vs normal, metastasis vs primary, *Twist1* vs non-*Twist1*, and normal lung vs normal liver comparisons from RNA-seq data. Lower right number indicates number of statistically insignificant genes. D) Venn diagram of statistically significant genes from tumor vs normal, metastasis vs primary, *Twist1* vs non-*Twist1*, and normal lung vs normal liver comparisons from integrated RNA-seq and proteomics data. Lower right number indicates number of statistically insignificant genes.

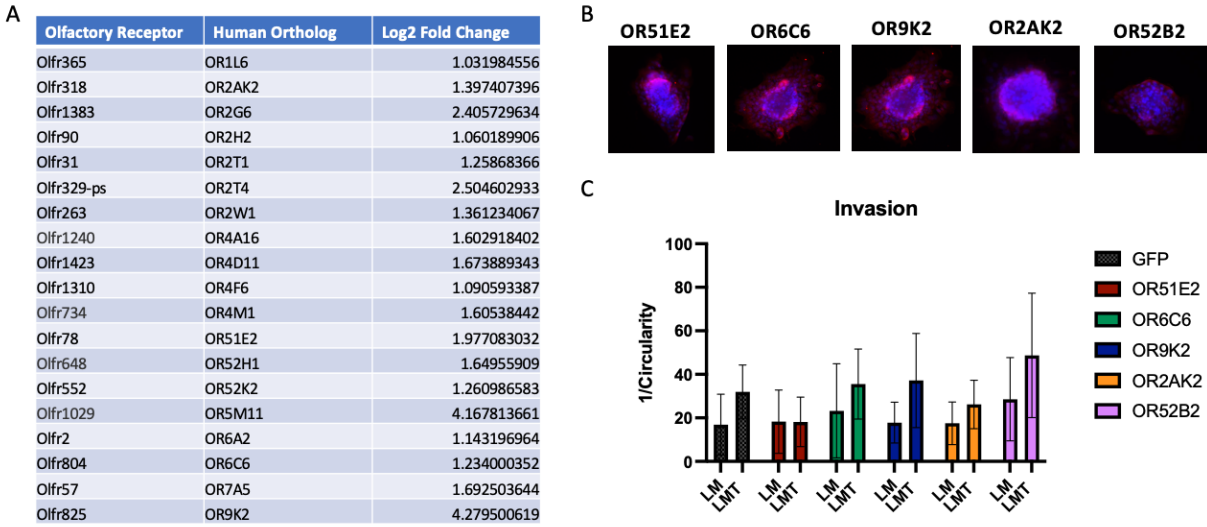| Olfactory Receptor	Human Ortholog	Log2 Fold Change
Olfr365	OR1L6	1.031984556
Olfr318	OR2AK2	1.397407396
Olfr1383	OR2G6	2.405729634
Olfr90	OR2H2	1.060189906
Olfr31	OR2T1	1.25868366
Olfr329-ps	OR2T4	2.504602933
Olfr263	OR2W1	1.361234067
Olfr1240	OR4A16	1.602918402
Olfr1423	OR4D11	1.673889343
Olfr1310	OR4F6	1.090593387
Olfr734	OR4M1	1.60538442
Olfr78	OR51E2	1.977083032
Olfr648	OR52H1	1.64955909
Olfr552	OR52K2	1.260986583
Olfr1029	OR5M11	4.167813661
Olfr2	OR6A2	1.143196964
Olfr804	OR6C6	1.234000352
Olfr57	OR7A5	1.692503644
Olfr825	OR9K2	4.279500619

Figure 2 Olfactory receptors are enriched in metastases.

A) Table of olfactory receptors that were overexpressed at least 2-fold in metastases vs the primary tumor and had a human ortholog. B) Overexpression of candidate olfactory receptors in HCC organoids was validated through immunofluorescent staining. C) Overexpression of candidate olfactory receptors did not significantly increase invasion in LM and LMT organoids.
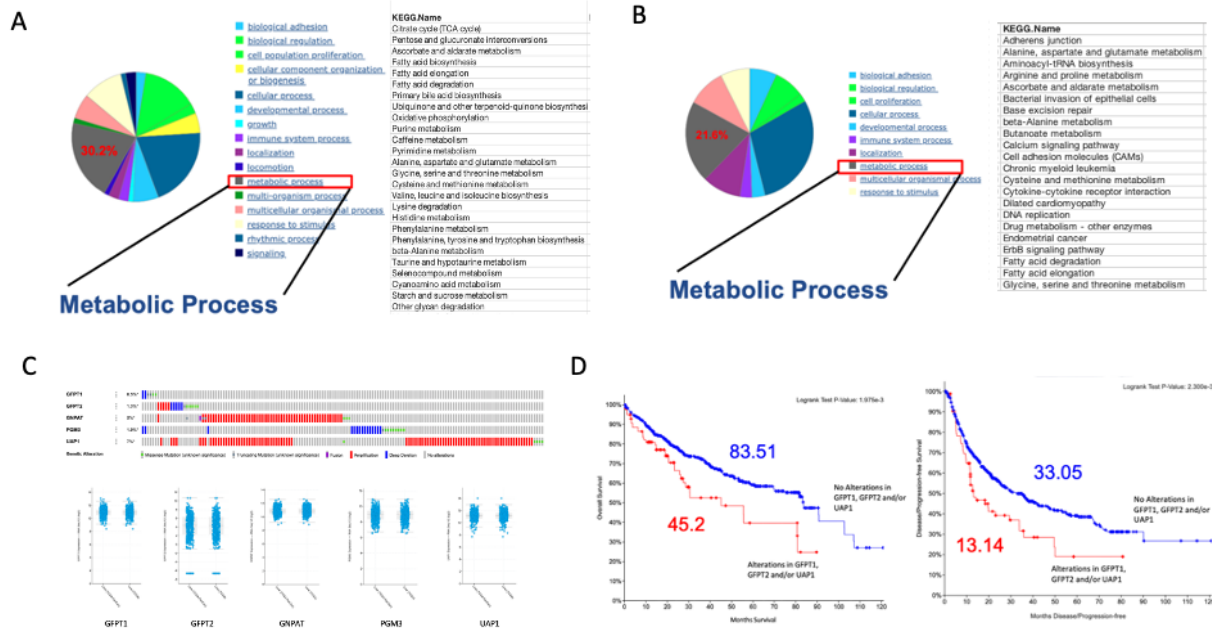
Figure 3 Metabolic processes are enriched in metastases.

A) Gene Ontology Enrichment Analysis revealed that genes of "Metabolic Process" represented 30.2% of differentially expressed genes between tumor vs normal, metastasis vs primary, and normal lung vs normal liver comparisons in the RNA-seq dataset. B) Gene Ontology Enrichment Analysis revealed that genes of "Metabolic Process" represented 21.6% of differentially expressed genes between tumor vs normal, metastasis vs primary, and normal lung vs normal liver comparisons in the integrated RNA-seq and mass spec dataset. C) HBP genes are frequently amplified in HCC patients and have high RNA expression levels. D) Kaplan-Meier estimates from cBioPortal show that HCC patients with alternations in GFPT2 and/or UAP1 (red) have worse median overall survival and disease/progression-free survival than HCC patients without alterations in GFPT2 and/or UAP1 (blue.)
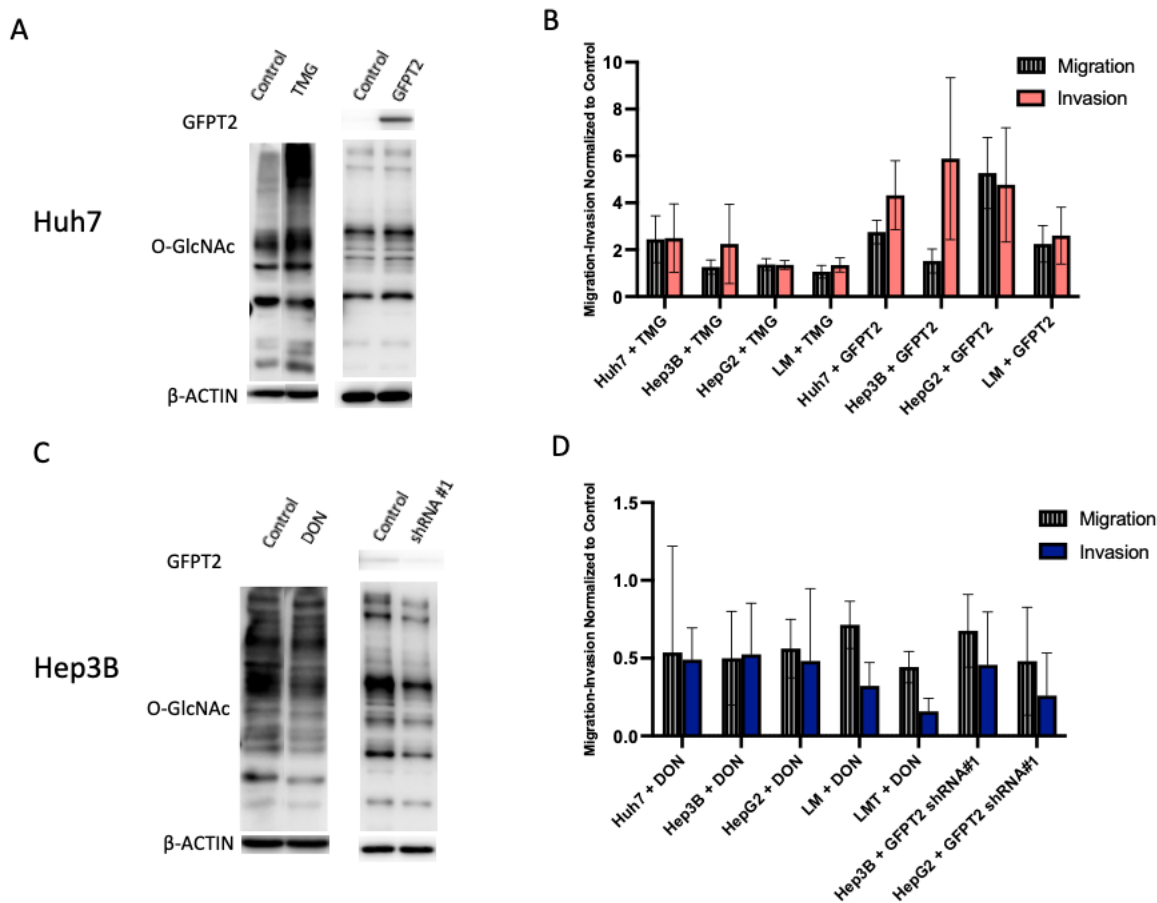
56

Figure 4 The HBP is sufficient and required for migration-invasion in vitro.

A) Representative Western blot showing that treatment with TMG and overexpression of GFPT2 increased global O-GlcNAcylation in a HCC cell line Huh7. B) Treatment with TMG and overexpression of GFPT2 increased migration (p=0.0374) and invasion (p=0.0087) across all HCC cell lines. C) Representative Western blot showing that treatment with DON and genetic knockdown of GFPT2 decreased global O-GlcNAcylation in a HCC cell line Hep3B. D) Treatment with DON or genetic knockdown of GFPT2 decreased migration (p<0.001) and invasion (p<0.001) across all HCC cell lines.
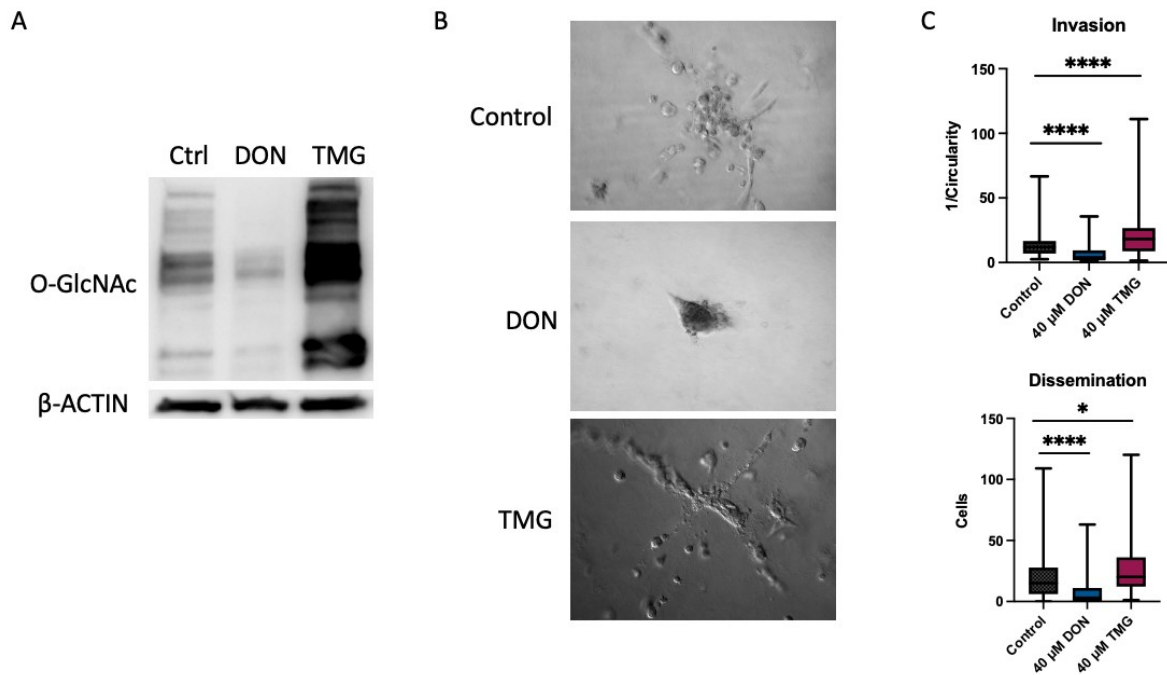
Figure 5.1 The HBP is sufficient and required for invasion and dissemination in LMT tumor organoids.

A) DON and TMG treatment decrease and increase, respectively, global O-GlcNAcylation in LMT organoids. B) Left: Representative DIC images show that DON decreases invasion and dissemination while TMG treatment increases invasion and dissemination. Right: Quantification of invasion and dissemination (n=3.)
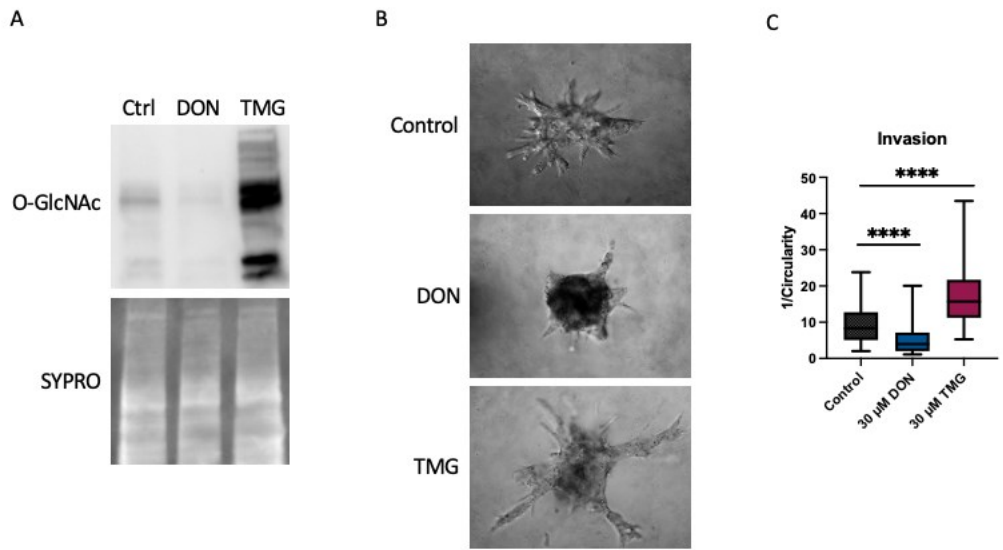
Figure 5.2 The HBP is sufficient and required for invasion and dissemination in LM tumor organoids.

A) DON and TMG treatment decrease and increase, respectively, global O-GlcNAcylation in LM organoids. B) Left: Representative DIC images show that DON decreases invasion while TMG treatment increases invasion. Right: Quantification of invasion (n=3.)
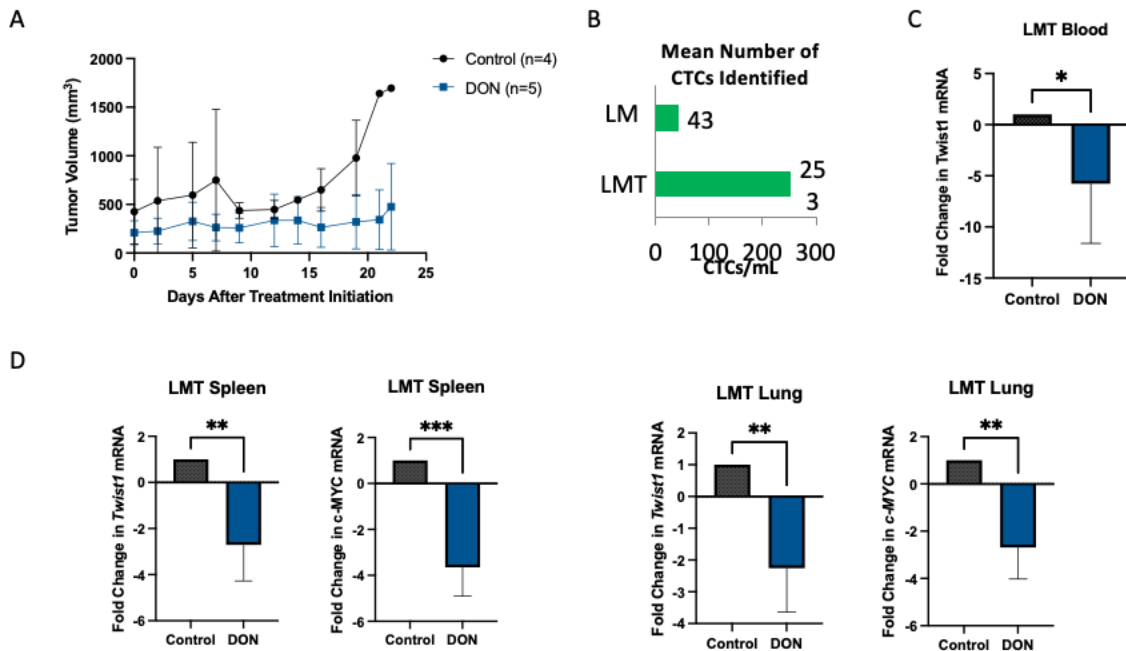
Figure 6 Targeting the HBP *in vivo* decreases tumor burden, circulating tumor cells, and colonization in distant organs.

A) 20mg/kg DON reduced tumor burden in a subcutaneous LMT model. B) Circulating tumor cells can be detected in LMT and LM whole blood. C) 20 mg/kg DON reduced circulating tumor cells in whole blood (n=6.) D) DON treatment decreased tumor cell colonization in the lung and spleen (n=4.)
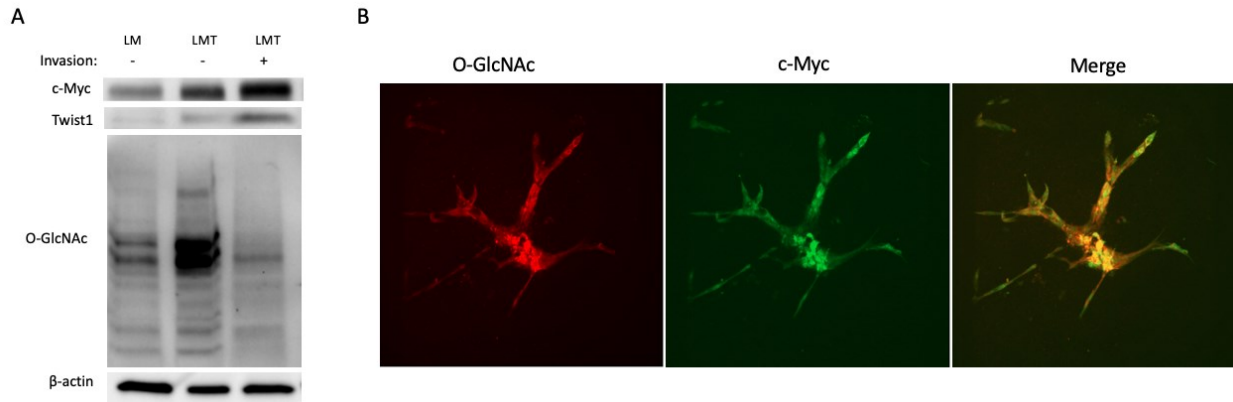
Figure 7 Pathways that may be regulated by the HBP during metastasis: c-MYC.

A) c-MYC protein levels are elevated in LMT vs LM tumor organoids and further increase with invasion. B) O-GlcNAc and c-MYC staining are stronger at the invasive leading edges of LMT organoid.
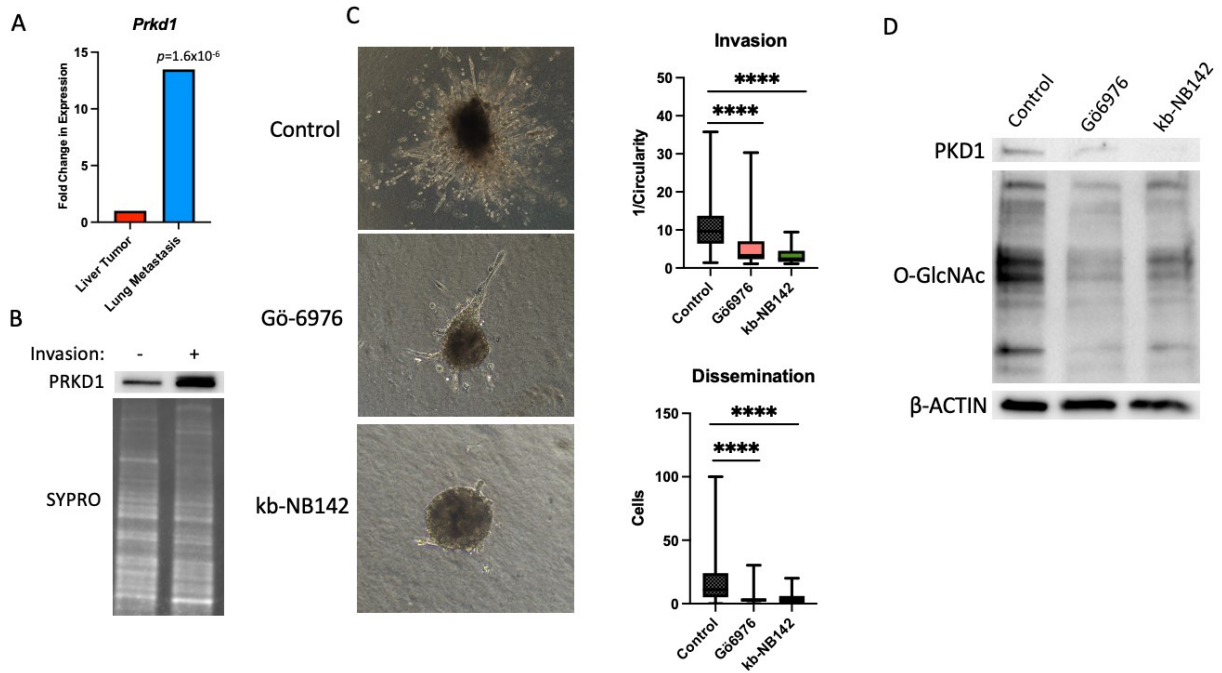
Figure 8 Pathways that may be regulated by the HBP during metastasis: PKD.

A) PKD mRNA levels were elevated in lung metastases vs primary liver tumor in the transcriptomic dataset. B) PKD1 protein levels increased in LMT organoids that were invading in collagen vs non-invading LMT organoids. C) Left: Representative DIC images of LMT organoids treated with 500 nM of the PKD1 inhibitors. Right: Quantification of invasion and dissemination (n=2.) D) PKD1 inhibitors decreased global O-GlcNAcylation in LMT organoids.

Figure 9 Pathways that may be regulated by the HBP during metastasis: HA.

A) GO overrepresentation pathway analysis from the transcriptomic dataset revealed that HA-related processes are specific to lung metastases vs primary tumor, liver tumor vs normal liver, and Twist vs nonTwist (indicated by a value of 1.) B) HAS1 is overexpressed in the lung metastases vs primary liver tumor. HA binding partner Cd44 is overexpressed in the lung vs liver. C) HAS1 and HAS2 are frequently amplified in HCC patients. Kaplan-Meier estimates show that HCC patients with genetic alterations in *HAS1, HAS2,* and/or *HAS3* (red) have significantly worse overall median survival compared to patients without these alterations (blue.)
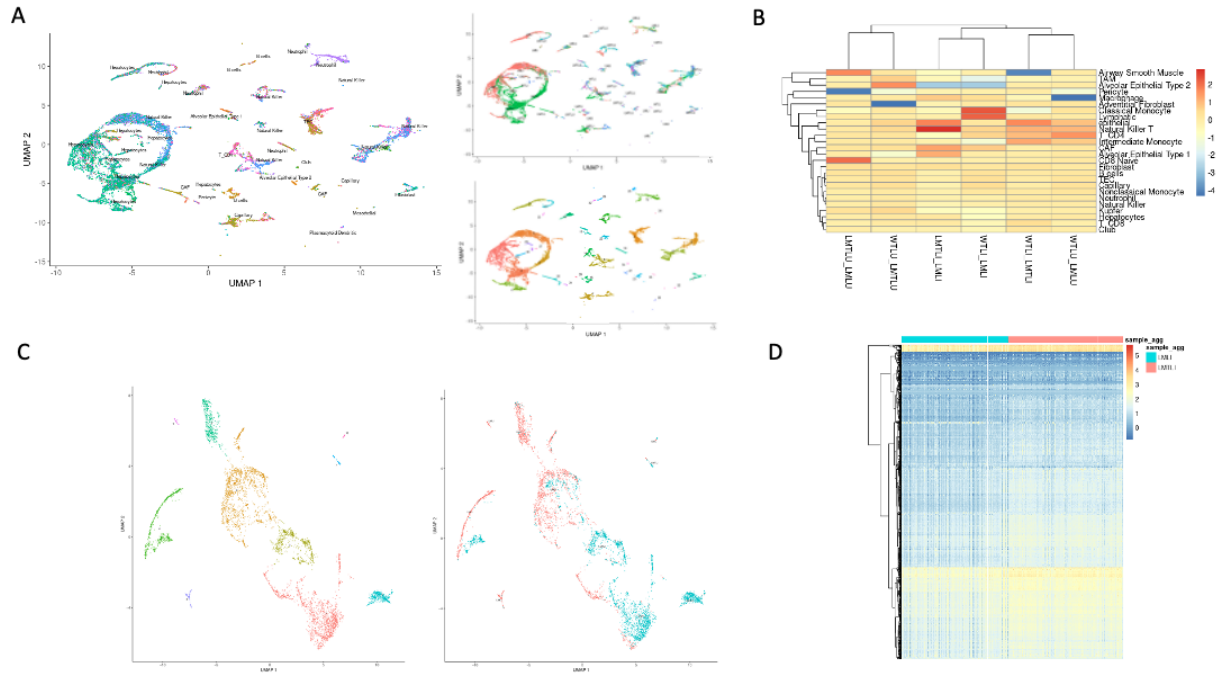
Figure 10.1: LMT and LM liver hepatocytes are distinct.

A) UMAP clustering and cell labeling of single cells from the lung and liver of LMT and LM mice. B) Overrepresented cell types across various comparisons. C) UMAP clustering of LMT and LM liver hepatocytes. D) Heatmap showing differential expression across LMT and LM hepatocytes. Genes are on y-axis and single cells on x-axis, separated by sample type.
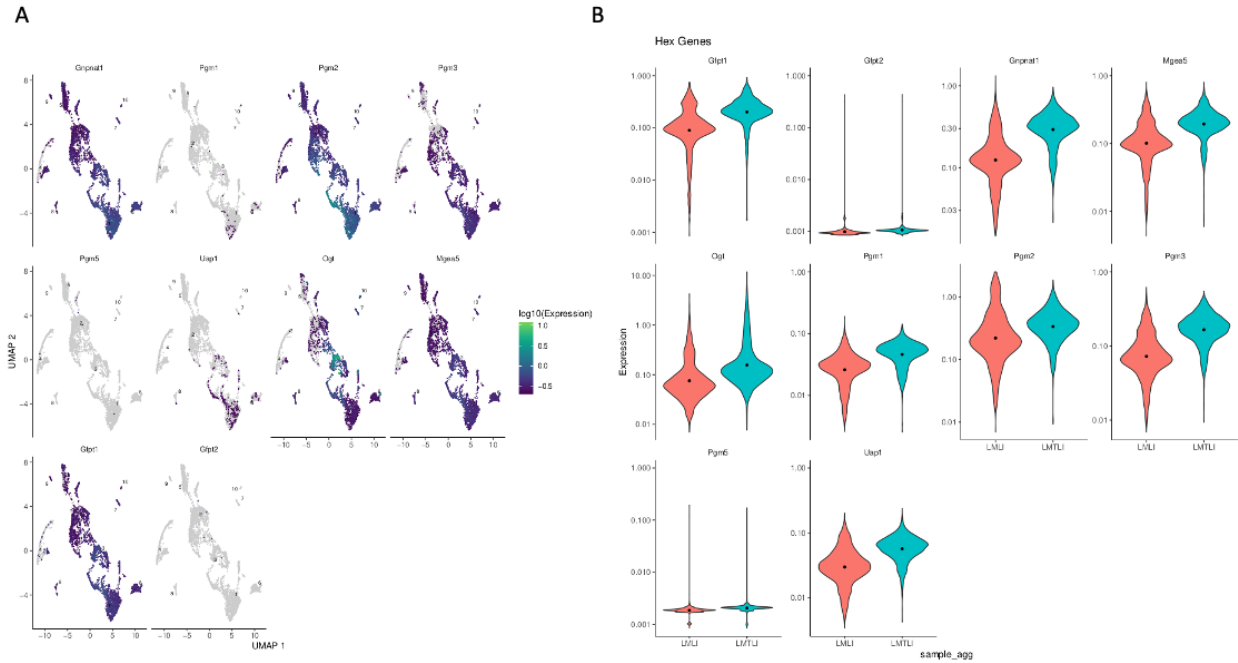
Figure 10.2 HBP genes are overexpressed in LMT liver hepatocytes.

A) UMAP showing expression levels of HBP genes in all liver hepatocytes. B) LMT liver hepatocytes (blue) have higher expression of HBP genes than LM liver hepatocytes (red.)
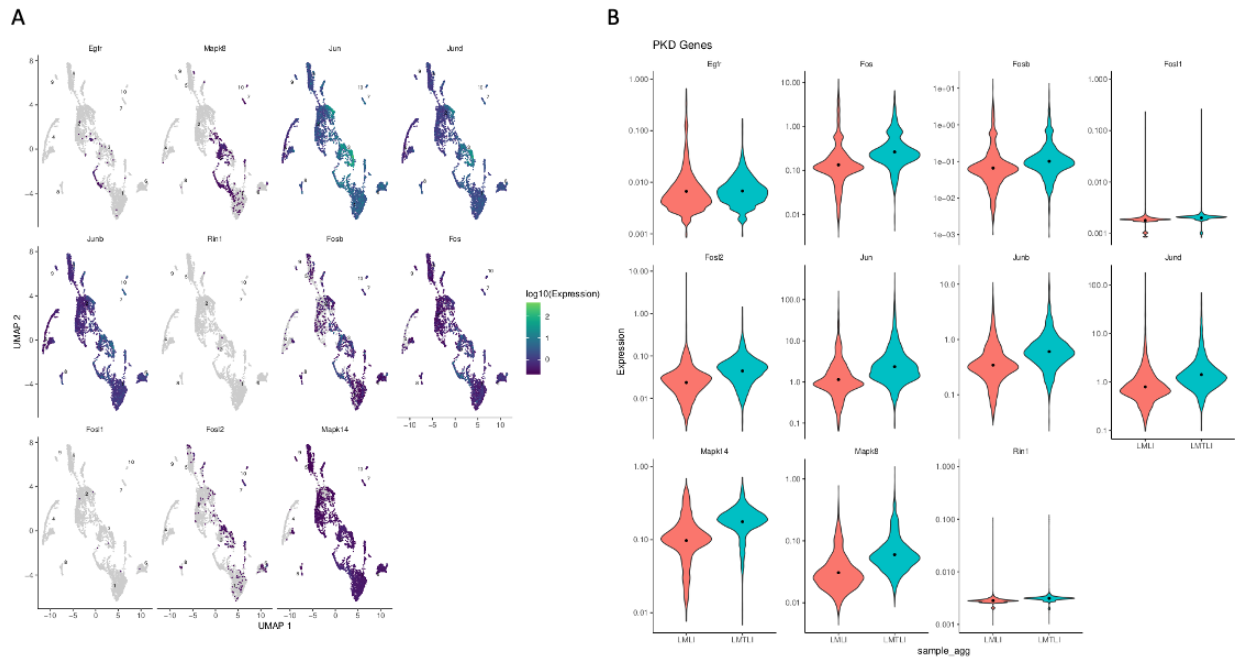
Figure 10.3 PKD pathway genes are overexpressed in LMT liver hepatocytes.

A) UMAP showing expression levels of PKD pathway genes in all liver hepatocytes. B) LMT liver hepatocytes (blue) have higher expression of PKD pathway genes than LM liver hepatocytes (red.)
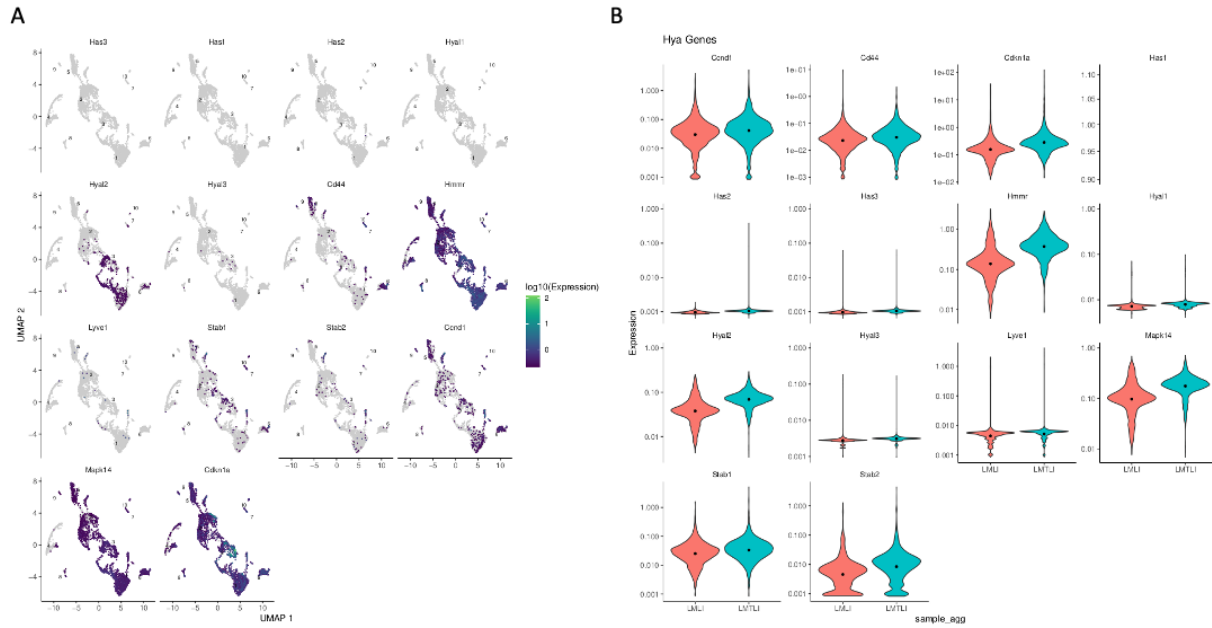
Figure 10.4 HA pathway genes are overexpressed in LMT liver hepatocytes.

A) UMAP showing expression levels of HA pathway genes in all liver hepatocytes. B) LMT liver hepatocytes (blue) have higher expression of HBP genes than LM liver hepatocytes (red.)
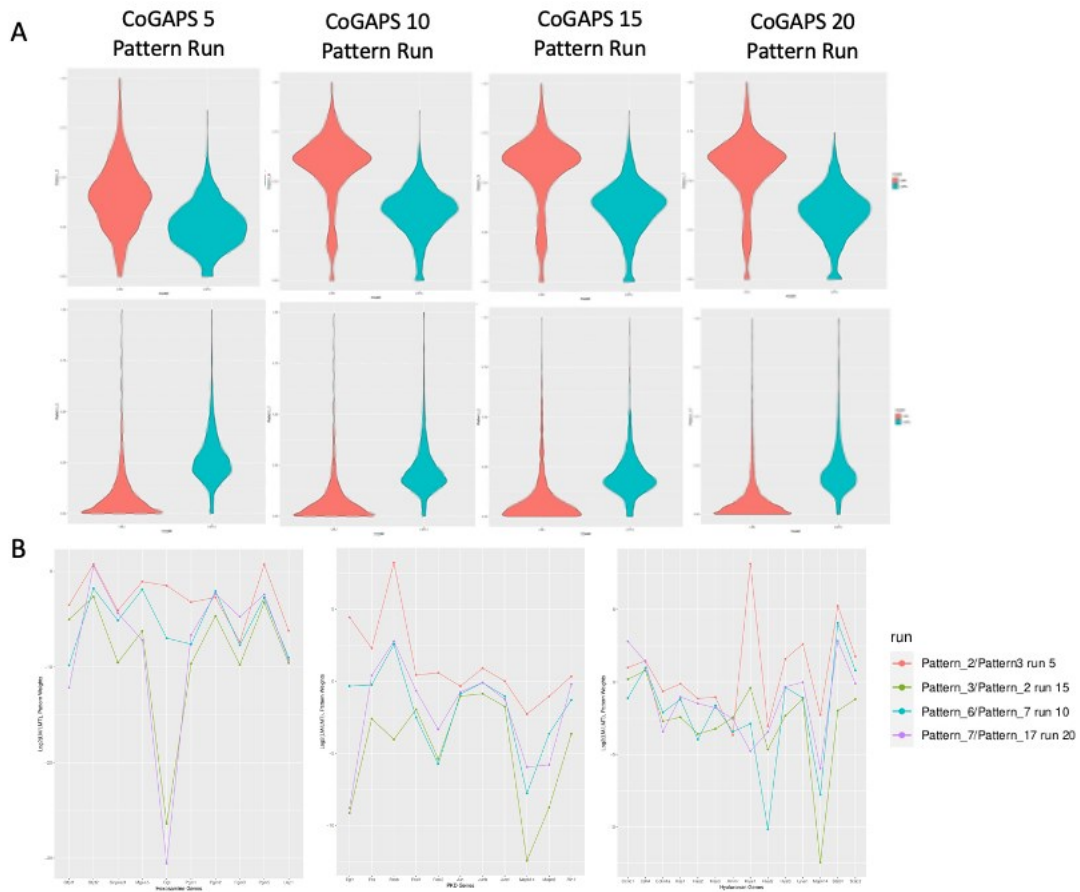
Figure 10.5 Genes in HBP, PKD, and HA pathways have higher weighting for LMT-associated patterns.

A) CoGAPS patterns that discriminate between LM and LMT liver hepatocytes were identified.

B) Genes in the hexosamine, PKD, and HA pathways show higher weighting for the LMT-associated patterns than the LM-associated patterns.

Chapter 3: Materials and methods

3.1 Cell lines and drug treatments

Huh7, Hep3B, and HepG2 cell lines were acquired from the American Type Culture Collection. LMT and LM cell lines were derived from the primary liver tumors of LMT and LM mice. Cell lines were cultured in Dulbecco's Modified Eagle Medium (Gibco, 11965118) with 10% FBS (GeminiBio) and 1% penicillin and streptomycin (Gibco, 15140122.) *In vitro* concentrations for 6-diazo-5-oxo-L-nor-Leucine (DON, Cayman Chemical, 17580) and Thiamet-G (TMG, Tocris, 4390) were determined through a dose titration from 10μm-60μm and used for subsequent migration-invasion assays.

In vitro migration-invasion assays

25,000 HCC cells were plated into Matrigel invasion chambers (Corning 354480) and control chambers (Corning 354578) in serum-free DMEM. DMEM with 10% FBS was added into wells as a chemoattractant. After 24 hours, chambers were fixed with methanol, stained with DAPI, and imaged. Cells were manually counted using ImageJ.

PCR genotyping

DNA was extracted from mouse tails by boiling 100 μL Solution A (0.5M EDTA pH8 and 10M NaOH in diH$_2$O) for one hour and then adding Solution B (Tris HCl pH 8 in diH$_2$O.) The *LAP-tTA (*L,*) tetO-Myc (*M,*) Twist1-tet-O-Luc (*T,*) Twist1DQD-tet-O-Luc (*DQD,*) and *Twist1F191G-tet-O-Luc (*F191G) transgenic lines were screened with the following primers. DNA was amplified by PCR, and PCR products were resolved on a 2% agarose gel.

LAP-tTA (L)	F	GCTGCTTAATGAGGTCGG
	R	CTCTGCACCTTGGTGATC
*tetO-Myc (*M)	F	CTGTATGTGGACGGCTTCTCG
	R	CTGCTGTCGTTGAGAGGGTAG
*Twist1-tetO-Luc (*T)	F	CTGAAGGATAAGTGACGAGCG
	R	CGACTGCTGCGTCTCTTGCGAG
*Twist1DQD-tetO-Luc (*DQD	F	TATCCAGATCCACCTTCG
	R	GTGCCAACCCTATTCTCCTTC
*Twist1F191G-tetO-Luc (*F191G)	F	CCCTGCGCAAGATCATCCC
	R	CAAACCTACAGGTGGGGTCT

Transgenic mice

LAP-tTA/tetO-Myc/Twist1-tetO-Luc (LMT) and *LAP-tTA/tetO-Myc* (LM) mice were taken off

doxycycline drinking water (2 mg/mL) at 5-8 weeks of age to induce transgene expression. After

4 weeks, luciferase expression in the abdomen of LMT mice was confirmed via bioluminescent

imaging (IVIS Spectrum In Vivo Imager, Johns Hopkins University Animal Facility.) DON was

administered intraperitoneal (I.P.) to LMT mice (20 mg/kg) twice a week for four weeks. All

procedures were performed in accordance with Stanford Administrative Panel on Lab Animal

Care (APLAC) and Johns Hopkins Animal Care and Use Committee (ACUC) protocols and animals were housed in a pathogen-free environment.

Subcutaneous mice

6-8 week old nude mice (Jackson Laboratories) were injected subcutaneously with 2 million LMT cells in 50% PBS and 50% Matrigel. Tumors formed around 5 days after injection. Once tumors reached a volume of 2-300 mm^3, DON treatment (20mg/kg IP twice a week) was initiated for 4 weeks. Tumor volume was measured three times a week.

CTC isolation and detection through SYBR-Green RT-qPCR

Whole blood was isolated from mice through cardiac puncture with 25G syringe needle coated with heparin sodium (Pfizer, NDC 0069-0058-02.) A density gradient was performed using Histopaque-1077 (Sigma 10771.) Total RNA was extracted from the buffy coat using Trizol (ThermoFisher Scientific 15596018) according to manufacturer protocol. cDNA was generated from 1μg of total RNA using the iScript cDNA synthesis kit (Bio-Rad 1708891) and amplified with iTaqTM Universal SYBR® Green Supermix (Bio-Rad 1725121) using the CFX384 Touch Real-Time PCR Detection System (Bio-Rad) for up to 40 cycles. PCR reactions were performed in quadruplicate in a final volume of 20μl. $2^{(-\Delta\Delta Ct)}$ method was used to determine relative fold gene expression.

Primers for qPCR are listed below:

HUMAN PRIMERS

MYC	F	TCCTCGGATTCTCTGCTCTC
	R	TCTTCCTCATCTTCTTGTTCCTC

MOUSE PRIMERS

Twist1	F	CTC GGA CAA GCT GAG CAA GA
	R	CTC CAT CCT CCA GAC GGA GA
Gapdh	F	AATGGTGAAGGTCGGTGTG
	R	GTGGAGTCATACTGGAACAGTAG

Viral transduction and shRNA transfection

Lentivirus was generated by transfecting HEK-293T cells with *GFPT2* shRNA construct and control GFP shRNA construct obtained from the Broad RNAi Consortium. HCC cell lines were then transduced with virus as previously described[20]. Early passage HCC cell lines (Huh7, Hep3B, HepG2, LM) were transfected with pWZL-Hygro vector (Ador pWZL- Hygro/*SNAI1* constructs, for two successive times over a 36-h period followed by selection, as previously described for Twist1 cell lines (Tran et al., 2012.)

Olfactory receptor transfection

OR6C6, OR9K2, and OR2AK2 open reading frame sequences were purchased from GenScript and cloned into the Lucy-Flag-Rho (LFR) vector provided by Dr. Jennifer Pluznick at Johns Hopkins University (Shepard et al., 2013.) LFR-OR51E2 and LFR-OR52B2 were provided by Dr. Pluznick. LFR-OR constructs were transfected into HCC organoids with Lipofectamine 2000 (Invitrogen 11668019) according to manufacturer protocol. 48 hrs after transfection, olfactory receptor expression was confirmed by immunofluorescent staining and organoids were plated for invasion assays.

Isolation and 3D culture of murine HCC tumor organoids

Organoids were isolated from LMT and LM liver tumors and plated for 3D collagen invasion and dissemination assays as previously described (Padmanaban et al., 2020.)

Immunoblot and immunofluorescence

Protein isolation and immunofluorescent staining on HCC organoids were performed as previously described.

HCC tumor organoids and cells were lysed in RIPA lysis buffer supplemented with Protease Inhibitor Cocktail (Sigma, P8340,) Phenylmethylsulfonyl fluoride (Sigma, 10837091001,) β-hexosamindase inhibitor (Millipore, 376820,) and Thiamet-G inhibitors. Cell lysates were sonicated with 5 second pulses and clarified by centrifugation. Protein concentrations were determined by Pierce BCA Protein Assay Kit (Thermo Scientific 23225.) 15-50μg of total

protein were resolved on 6-12% SDS-polyacrylamide gels and transferred to PVDF membranes.

Antigen detection was carried out with antibodies against the following proteins:

Antibody	Vendor	Catalog No.
O-GlcNAc (CTD 110.6) Mouse Ab	Cell Signaling Technology	9875
c-Myc (Y69)	AbCam	Ab32072
β-actin (C4)	Santa Cruz Biotechnology	Sc-47778
PKCμ	AbCam	Ab131460
GFPT2	Abcam	Ab190966
FLAG	Sigma Aldrich	F3165

RNA isolation for RNA-seq

Mouse tissue was cryo-pulverized and RNA isolated with RNeasy Mini Kit (Qiagen 74104) according to manufacturer protocol. RIN analysis and RNA-seq was performed by the JHU GRCF Core.

RNA-seq analysis

FASTQ files from RNA-seq were processed into read counts with salmon (https://www.ncbi.nlm.nih.gov/pmc/articles/PMC5600148/) and tximport (https://f1000research.com/articles/4-1521,) using mouse genome mm10. Variance stabilization was performed with rlog, principal component analysis, and differential expression analysis through DESeq2 (https://genomebiology.biomedcentral.com/articles/10.1186/s13059-014-0550-8.) Genes with absolute log fold change greater than 1 and FDR adjusted p-value below 0.05 are called significantly differentially expressed. ComplexHeatmap (https://academic.oup.com/bioinformatics/article/32/18/2847/1743594) is used to generate heat maps of z-scored, variance stabilized gene expression for genes that are differentially expressed

between metastasis samples and primary tumors, but not between corresponding normal tissues from the same tissue sites. Pathway analysis was performed on Hallmark, KEGG, and GO pathways from MSigDB (https://www.ncbi.nlm.nih.gov/pmc/articles/PMC3106198/) with an overrepresentation test in the R package GeneOverlap.

Protein extraction, digestion, and labeling for mass spectrometry

Mouse tissue samples were sonicated in 8 M urea and 50 mM triethylammonium bicarbonate (TEABC) with 35% amplitude for 1 min. Protein lysates were centrifuged at 16,000 x g at 4 °C to exclude cell debris and protein concentration was estimated using BCA assay. A total of 200 µg of each sample was reduced with 10 mM dithiothreitol at room temperature for one hour and alkylated with 30 mM iodoacetamide for 20 minutes in the dark. The protein samples were digested with Lys-C (1:100) at 37 °C for 3 h followed by sequencing-grade trypsin (1:50) overnight at 37 °C. The resulting peptides were subject to desalting and labeling with 10-plex TMT reagents according to the manufacturer's instructions (Thermo Fisher Scientific.) The labeling reaction was performed for one hour at room temperature, followed by quenching with 100 mM Tris-HCl (pH 8.0.) The digested and labeled peptides were pooled and desalted with SEP-PAK C18 (Waters Corporation, Milford, MA.) The peptides were fractionated by basic pH reversed-phase liquid chromatography (bRPLC) into 96 fractions, followed by concatenation into 24 fractions by combining every 24th fractions. Briefly, Agilent 1260 offline LC system was used for bRPLC fractionation, which includes a binary pump, VWD detector, an autosampler, and an automatic fraction collector. In brief, lyophilized samples were reconstituted in solvent A (10 mM triethylammonium bicarbonate, pH 8.5) and loaded onto XBridge C18, 5 µm 250 × 4.6 mm column (Waters, Milford, MA.) Peptides were resolved using a gradient of 3 to 50% solvent

B (10 mM triethylammonium bicarbonate in acetonitrile, pH 8.5) at a flow rate of 1 ml per min

over 50 min collecting 96 fractions. Subsequently, the fractions were concatenated into 12

fractions followed by vacuum drying using a SpeedVac.

Mass spectrometry

The fractionated peptides were analyzed on an Orbitrap Fusion Lumos Tribrid Mass

Spectrometer coupled with the EASY-nLC 1200 nano-flow liquid chromatography system

(Thermo Fisher Scientific.) The peptides from each fraction were reconstituted in 15 μl 0.1%

formic acid and all the 15 μl were loaded on an Acclaim PepMap100 Nano-Trap Column

(100 μm × 2 cm, Thermo Fisher Scientific) packed with 5 μm C18 particles at a flow rate of 5 μl

per minute. Peptides were resolved at 250-nl/min

flow rate using a linear gradient of 10% to 35% solvent B (0.1% formic acid in 95% acetonitrile)

over 95 minutes on an EASY-Spray column (50 cm x 75 μm ID, Thermo Fisher

Scientific)packed with 2 μm C18 particles, which was fitted with an EASY-Spray ion source that

was operated at a voltage of 2.0 kV.

Mass spectrometry analysis was carried out in a data-dependent manner with a full scan in the

mass-to-charge ratio (m/z) range of 350 to 1550 in the "Top Speed" setting, three seconds per

cycle. MS1, MS2 and MS3 were acquired for the peptide fragmentation ions in MS2 level and

the reporter ions in MS3 level. MS1 scans were measured at a resolution of 120,000 at an m/z of

200. MS2 scan were acquired by fragmenting precursor ions using the higher-energy collisional

dissociation (HCD) method and detected at a mass resolution of 30,000, at an m/z of 200. MS3

scan were acquired by isolating top 5 fragment ions monitored in MS2 scan and fragmenting the

top 5 selected ions using the higher-energy collisional dissociation method and detected at a mass resolution of 30,000, at an m/z of 200. Automatic gain control for MS1 was set to one million ions and for MS2 and MS3 was set to 0.05 million ions. A maximum ion injection time was set to 50 ms for MS1 and 100 ms for MS2 and MS3. MS1 was acquired in profile mode and MS2 and MS3 were acquired in centroid mode. Higher-energy collisional dissociation was set to 35 for MS2 and 65 for MS3. Dynamic exclusion was set to 30 seconds, and singly-charged ions were rejected. Internal calibration was carried out using the lock mass option (m/z 445.1200025) from ambient air.

Proteomics data analysis

Proteomics data were pre-processed into abundance counts. Loess normalization and ComBat (https://www.ncbi.nlm.nih.gov/pmc/articles/PMC3307112/) is performed on log transformed protein abundances to adjust for batch effects between sets. Differential expression analysis on the batch corrected data is performed with LIMMA (https://academic.oup.com/nar/article/43/7/e47/2414268,) with proteins with absolute log fold change greater than 1 and FDR adjusted p-value below 0.05 called statistically significant.

Immediate tumor dissociation and immediate single cell library preparation

Dissociation was performed using the Mouse Liver Tumor Dissociation Kit (Miltenyi Biotec) following manufacturer's instructions. Briefly, the samples were minced with scalpels and digested in an enzyme mix containing collagenase during an incubation at 37C for approximately 40 minutes in the gentleMACS Octo Dissociator with Heaters (Miltenyi Biotec.) At the end of

the incubation, the dissociated tissue was filtered using a 40mm strainer to remove debris. In order to remove red cells, ACK Lysing Buffer (Gibco) was used. Cell counting and viability was performed with Trypan Blue (Invitrogen) using a hemocytometer.

Single cell and single nuclei sequencing

The 10X Genomics Chromium Single Cell platform was used for the single cell sequencing libraries preparations. Single cell gene expression sequencing library preparations used the Chromium Single Cell 3' Library & Gel Bead Kit, following manufacturer's instructions. A total of 17,000 cells were loaded for each sample in order to recover the transcripts of approximately 10,000 cells. Samples were sequenced using the NovaSeq (Illumina) with a depth of 50,000 reads per cell and following 10X Genomics established parameters. Sequencing was performed at the Experimental and Computational Genomics Core at the Sidney Kimmel Comprehensive Cancer Center.

High-throughput analysis

ScRNAseq data was preprocessed with CellRanger (10x Genomics) for gene level counts with prebuilt human (GRCh38) references. Cells were filtered based on quality control metrics including empty cells, doublets, and mitochondrial gene expression with Seurat. Genes detected in fewer than 10% of cells were filtered prior to analysis. Subsequent analyses of cell type identification and differential expression analysis were performed with Monocole3. Cell types were identified from the scRNAseq data through clustering and analysis of marker genes of the subclusters. Additional analysis of the copy number of epithelial cells with inferCNV were used to delineate tumor cells from normal epithelial cells. Specific focus was given to the gene

markers previously used to annotate cell types from HCC single cell datasets. Additional functional analysis of pathways was assessed with the fGSEA package for molecular signaling pathways in MsigDB. Finally, the Bayesian non-negative matrix factorization method CoGAPS will be applied to assess common gene expression patterns across all cell types, as well as cell type specific patterns.

Chapter 4: Discussion

Metabolic processes are enriched in lung metastases in a *Twist1*-dependent metastasis mouse model of *MYC*-induced HCC. The hexosamine biosynthetic pathway is required and sufficient for migration-invasion, dissemination, and colonization *in vitro* in HCC cell lines, *ex vivo* in HCC organoids, and *in vivo* in GEMM model of *MYC*-induced HCC. Increased HBP O-GlcNAcylation may increase levels of PKD, HA, and c-MYC. scRNA-seq shows that LMT liver hepatocytes have higher gene expression amongst genes associated with the HBP, PKD, and HA pathways. The HBP may be a potential therapeutic target for advanced HCC patients.

References

[1]D. Hanahan, R.A. Weinberg, Hallmarks of cancer: the next generation. Cell 144 (2011) 646-674.

[2]M.V. Liberti, J.W. Locasale, The Warburg Effect: How Does it Benefit Cancer Cells? Trends Biochem Sci 41 (2016) 211-218.

[3]J. Zheng, Energy metabolism of cancer: Glycolysis versus oxidative phosphorylation (Review.) Oncol Lett 4 (2012) 1151-1157.

[4]R.J. DeBerardinis, Is cancer a disease of abnormal cellular metabolism? New angles on an old idea. Genet Med 10 (2008) 767-777.

[5]J. Jia, F. Zhu, X. Ma, Z. Cao, Y. Li, Y.Z. Chen, Mechanisms of drug combinations: interaction and network perspectives. Nat Rev Drug Discov 8 (2009) 111-128.

[6]C.M. Metallo, M.G. Vander Heiden, Metabolism strikes back: metabolic flux regulates cell signaling. Genes Dev 24 (2010) 2717-2722.

[7]J.A. Hanover, M.W. Krause, D.C. Love, Bittersweet memories: linking metabolism to epigenetics through O-GlcNAcylation. Nat Rev Mol Cell Biol 13 (2012) 312-321.

[8]K. Vaidyanathan, S. Durning, L. Wells, Functional O-GlcNAc modifications: implications in molecular regulation and pathophysiology. Crit Rev Biochem Mol Biol 49 (2014) 140-163.

[9]S. Marshall, V. Bacote, R.R. Traxinger, Discovery of a metabolic pathway mediating glucose-induced desensitization of the glucose transport system. Role of hexosamine biosynthesis in the induction of insulin resistance. J Biol Chem 266 (1991) 4706-4712.

[10]M.R. Bond, J.A. Hanover, A little sugar goes a long way: the cell biology of O-GlcNAc. J Cell Biol 208 (2015) 869-880.

[11]J. Munkley, I.G. Mills, D.J. Elliott, The role of glycans in the development and progression of prostate cancer. Nat Rev Urol 13 (2016) 324-333.

[12]J.K. Sethi, A.J. Vidal-Puig, Wnt signalling at the crossroads of nutritional regulation. Biochem J 416 (2008) e11-13.

[13]T. Dong, X. Kang, Z. Liu, S. Zhao, W. Ma, Q. Xuan, H. Liu, Z. Wang, Q. Zhang, Altered glycometabolism affects both clinical features and prognosis of triple-negative and neoadjuvant chemotherapy-treated breast cancer. Tumour biology : the journal of the International Society for Oncodevelopmental Biology and Medicine 37 (2016) 8159-8168.
[14]C. Yang, P. Peng, L. Li, M. Shao, J. Zhao, L. Wang, F. Duan, S. Song, H. Wu, J. Zhang, R. Zhao, D. Jia, M. Zhang, W. Wu, C. Li, Y. Rong, L. Zhang, Y. Ruan, J. Gu, High expression of GFAT1 predicts poor prognosis in patients with pancreatic cancer. Sci Rep 6 (2016) 39044.

[15]L. Li, M. Shao, P. Peng, C. Yang, S. Song, F. Duan, D. Jia, M. Zhang, J. Zhao, R. Zhao, W. Wu, L. Wang, C. Li, H. Wu, J. Zhang, X. Wu, Y. Ruan, J. Gu, High expression of GFAT1 predicts unfavorable prognosis in patients with hepatocellular carcinoma. Oncotarget 8 (2017) 19205-19217.

[16]H.J. Johansson, B.C. Sanchez, J. Forshed, O. Stal, H. Fohlin, R. Lewensohn, P. Hall, J. Bergh, J. Lehtio, B.K. Linderholm, Proteomics profiling identify CAPS as a potential predictive marker of tamoxifen resistance in estrogen receptor positive breast cancer. Clin Proteomics 12 (2015) 8.

[17]J.H. Ji, Y.L. Oh, M. Hong, J.W. Yun, H.W. Lee, D. Kim, Y. Ji, D.H. Kim, W.Y. Park, H.T. Shin, K.M. Kim, M.J. Ahn, K. Park, J.M. Sun, Identification of Driving ALK Fusion Genes and Genomic Landscape of Medullary Thyroid Cancer. PLoS Genet 11 (2015) e1005467.

[18]H. Ying, A.C. Kimmelman, C.A. Lyssiotis, S. Hua, G.C. Chu, E. Fletcher-Sananikone, J.W. Locasale, J. Son, H. Zhang, J.L. Coloff, H. Yan, W. Wang, S. Chen, A. Viale, H. Zheng, J.H. Paik, C. Lim, A.R. Guimaraes, E.S. Martin, J. Chang, A.F. Hezel, S.R. Perry, J. Hu, B. Gan, Y. Xiao, J.M. Asara, R. Weissleder, Y.A. Wang, L. Chin, L.C. Cantley, R.A. DePinho, Oncogenic Kras maintains pancreatic tumors through regulation of anabolic glucose metabolism. Cell 149 (2012) 656-670.

[19]B. Liu, Z.B. Huang, X. Chen, Y.X. See, Z.K. Chen, H.K. Yao, Mammalian Target of Rapamycin 2 (MTOR2) and C-MYC Modulate Glucosamine-6-Phosphate Synthesis in Glioblastoma (GBM) Cells Through Glutamine: Fructose-6-Phosphate Aminotransferase 1 (GFAT1.) Cellular and molecular neurobiology 39 (2019) 415-434.

[20]C. Phoomak, K. Vaeteewoottacharn, A. Silsirivanit, C. Saengboonmee, W. Seubwai, K. Sawanyawisuth, C. Wongkham, S. Wongkham, High glucose levels boost the aggressiveness of highly metastatic cholangiocarcinoma cells via O-GlcNAcylation. Sci Rep 7 (2017) 43842.

[21]M. Shimizu, N. Tanaka, IL-8-induced O-GlcNAc modification via GLUT3 and GFAT regulates cancer stem cell-like properties in colon and lung cancer cells. Oncogene 38 (2019) 1520-1533.

[22]S. Oikari, T. Kettunen, S. Tiainen, J. Hayrinen, A. Masarwah, M. Sudah, A. Sutela, R. Vanninen, M. Tammi, P. Auvinen, UDP-sugar accumulation drives hyaluronan synthesis in breast cancer. Matrix biology : journal of the International Society for Matrix Biology 67 (2018) 63-74.

[23]T. Chanmee, P. Ontong, T. Izumikawa, M. Higashide, N. Mochizuki, C. Chokchaitaweesuk, M. Khansai, K. Nakajima, I. Kakizaki, P. Kongtawelert, N. Taniguchi, N. Itano, Hyaluronan Production Regulates Metabolic and Cancer Stem-like Properties of Breast Cancer Cells via Hexosamine Biosynthetic Pathway-coupled HIF-1 Signaling. J Biol Chem 291 (2016) 24105-24120.

[24]H.M. Itkonen, S. Minner, I.J. Guldvik, M.J. Sandmann, M.C. Tsourlakis, V. Berge, A. Svindland, T. Schlomm, I.G. Mills, O-GlcNAc transferase integrates metabolic pathways to regulate the stability of c-MYC in human prostate cancer cells. Cancer Res 73 (2013) 5277-5287.

[25]A.K. Kaushik, A. Shojaie, K. Panzitt, R. Sonavane, H. Venghatakrishnan, M. Manikkam, A. Zaslavsky, V. Putluri, V.T. Vasu, Y. Zhang, A.S. Khan, S. Lloyd, A.T. Szafran, S. Dasgupta, D.A. Bader, F. Stossi, H. Li, S. Samanta, X. Cao, E. Tsouko, S. Huang, D.E. Frigo, L. Chan, D.P. Edwards, B.A. Kaipparettu, N. Mitsiades, N.L. Weigel, M. Mancini, S.E. McGuire, R. Mehra, M.M. Ittmann, A.M. Chinnaiyan, N. Putluri, G.S. Palapattu, G. Michailidis, A. Sreekumar, Inhibition of the hexosamine biosynthetic pathway promotes castration-resistant prostate cancer. Nat Commun 7 (2016) 11612.

[26]K. Taparra, H. Wang, R. Malek, A. Lafargue, M.A. Barbhuiya, X. Wang, B.W. Simons, M. Ballew, K. Nugent, J. Groves, R.D. Williams, T. Shiraishi, J. Verdone, G. Yildirir, R. Henry, B. Zhang, J. Wong, K.K. Wang, B.D. Nelkin, K.J. Pienta, D. Felsher, N.E. Zachara, P.T. Tran, O-GlcNAcylation is required for mutant KRAS-induced lung tumorigenesis. The Journal of clinical investigation 128 (2018) 4924-4937.

[27]W. Zhang, G. Bouchard, A. Yu, M. Shafiq, M. Jamali, J.B. Shrager, K. Ayers, S. Bakr, A.J. Gentles, M. Diehn, A. Quon, R.B. West, V. Nair, M. van de Rijn, S. Napel, S.K. Plevritis, GFPT2-Expressing Cancer-Associated Fibroblasts Mediate Metabolic Reprogramming in Human Lung Adenocarcinoma. Cancer Res 78 (2018) 3445-3457.

[28]J. Wang, X. Liu, Y.H. Liang, L.F. Li, X.D. Su, Acceptor substrate binding revealed by crystal structure of human glucosamine-6-phosphate N-acetyltransferase 1. FEBS Lett 582 (2008) 2973-2978.

[29]M. Zhao, H. Li, Y. Ma, H. Gong, S. Yang, Q. Fang, Z. Hu, Nanoparticle abraxane possesses impaired proliferation in A549 cells due to the underexpression of glucosamine 6-phosphate N-acetyltransferase 1 (GNPNAT1/GNA1.) International journal of nanomedicine 12 (2017) 1685-1697.

[30]M.J. Marshall, F.E. Neal, D.M. Goldberg, Isoenzymes of hexokinase, 6-phosphogluconate dehydrogenase, phosphoglucomutase and lactate dehydrogenase in uterine cancer. Br J Cancer 40 (1979) 380-390.

[31]C.H. Lee, S.J. Jeong, S.M. Yun, J.H. Kim, H.J. Lee, K.S. Ahn, S.H. Won, H.S. Kim, H.J. Lee, K.S. Ahn, S. Zhu, C.Y. Chen, S.H. Kim, Down-regulation of phosphoglucomutase 3 mediates sulforaphane-induced cell death in LNCaP prostate cancer cells. Proteome Sci 8 (2010) 67.

[32]J. Munkley, D. Vodak, K.E. Livermore, K. James, B.T. Wilson, B. Knight, P. McCullagh, J. McGrath, M. Crundwell, L.W. Harries, H.Y. Leung, C.N. Robson, I.G. Mills, P. Rajan, D.J. Elliott, Glycosylation is an Androgen-Regulated Process Essential for Prostate Cancer Cell Viability. EBioMedicine 8 (2016) 103-116.

[33]F. Ricciardiello, G. Votta, R. Palorini, I. Raccagni, L. Brunelli, A. Paiotta, F. Tinelli, G. D'Orazio, S. Valtorta, L. De Gioia, R. Pastorelli, R.M. Moresco, B. La Ferla, F. Chiaradonna, Inhibition of the Hexosamine Biosynthetic Pathway by targeting PGM3 causes breast cancer growth arrest and apoptosis. Cell death & disease 9 (2018) 377.

[34]F. Ricciardiello, Y. Gang, R. Palorini, Q. Li, M. Giampa, F. Zhao, L. You, B. La Ferla, H. De Vitto, W. Guan, J. Gu, T. Zhang, Y. Zhao, F. Chiaradonna, Hexosamine pathway inhibition overcomes pancreatic cancer resistance to gemcitabine through unfolded protein response and EGFR-Akt pathway modulation. Oncogene 39 (2020) 4103-4117.

[35]M. Albitar, W. Ma, L. Lund, F. Albitar, K. Diep, H.A. Fritsche, N. Shore, Predicting Prostate Biopsy Results Using a Panel of Plasma and Urine Biomarkers Combined in a Scoring System. J Cancer 7 (2016) 297-303.

[36]H.M. Itkonen, N. Engedal, E. Babaie, M. Luhr, I.J. Guldvik, S. Minner, J. Hohloch, M.C. Tsourlakis, T. Schlomm, I.G. Mills, UAP1 is overexpressed in prostate cancer and is protective against inhibitors of N-linked glycosylation. Oncogene 34 (2015) 3744-3750.

[37]R. Shafi, S.P. Iyer, L.G. Ellies, N. O'Donnell, K.W. Marek, D. Chui, G.W. Hart, J.D. Marth, The O-GlcNAc transferase gene resides on the X chromosome and is essential for embryonic stem cell viability and mouse ontogeny. Proc Natl Acad Sci U S A 97 (2000) 5735-5739.

[38]W.A. Lubas, J.A. Hanover, Functional expression of O-linked GlcNAc transferase. Domain structure and substrate specificity. J Biol Chem 275 (2000) 10983-10988.

[39]S.A. Caldwell, S.R. Jackson, K.S. Shahriari, T.P. Lynch, G. Sethi, S. Walker, K. Vosseller, M.J. Reginato, Nutrient sensor O-GlcNAc transferase regulates breast cancer tumorigenesis through targeting of the oncogenic transcription factor FoxM1. Oncogene 29 (2010) 2831-2842.

[40]C.M. Ferrer, T.P. Lynch, V.L. Sodi, J.N. Falcone, L.P. Schwab, D.L. Peacock, D.J. Vocadlo, T.N. Seagroves, M.J. Reginato, O-GlcNAcylation regulates cancer metabolism and survival stress signaling via regulation of the HIF-1 pathway. Mol Cell 54 (2014) 820-831.

[41]V.L. Sodi, S. Khaku, R. Krutilina, L.P. Schwab, D.J. Vocadlo, T.N. Seagroves, M.J. Reginato, mTOR/MYC Axis Regulates O-GlcNAc Transferase Expression and O-GlcNAcylation in Breast Cancer. Mol Cancer Res 13 (2015) 923-933.

[42]C.M. Ferrer, T.Y. Lu, Z.A. Bacigalupa, C.D. Katsetos, D.A. Sinclair, M.J. Reginato, O-GlcNAcylation regulates breast cancer metastasis via SIRT1 modulation of FOXM1 pathway. Oncogene (2016) 228.

[43]A. Barkovskaya, K. Seip, B. Hilmarsdottir, G.M. Maelandsmo, S.A. Moestue, H.M. Itkonen, O-GlcNAc Transferase Inhibition Differentially Affects Breast Cancer Subtypes. Sci Rep 9 (2019) 5670.

[44]T. Kamigaito, T. Okaneya, M. Kawakubo, H. Shimojo, O. Nishizawa, J. Nakayama, Overexpression of O-GlcNAc by prostate cancer cells is significantly associated with poor prognosis of patients. Prostate Cancer Prostatic Dis 17 (2014) 18-22.

[45]T.P. Lynch, C.M. Ferrer, S.R. Jackson, K.S. Shahriari, K. Vosseller, M.J. Reginato, Critical role of O-Linked beta-N-acetylglucosamine transferase in prostate cancer invasion, angiogenesis, and metastasis. J Biol Chem 287 (2012) 11070-11081.

[46]H.M. Itkonen, S.S. Gorad, D.Y. Duveau, S.E. Martin, A. Barkovskaya, T.F. Bathen, S.A. Moestue, I.G. Mills, Inhibition of O-GlcNAc transferase activity reprograms prostate cancer cell metabolism. Oncotarget 7 (2016) 12464-12476.

[47]Q. Zhu, L. Zhou, Z. Yang, M. Lai, H. Xie, L. Wu, C. Xing, F. Zhang, S. Zheng, O-GlcNAcylation plays a role in tumor recurrence of hepatocellular carcinoma following liver transplantation. Med Oncol 29 (2012) 985-993.

[48]C. Guinez, G. Filhoulaud, F. Rayah-Benhamed, S. Marmier, C. Dubuquoy, R. Dentin, M. Moldes, A.F. Burnol, X. Yang, T. Lefebvre, J. Girard, C. Postic, O-GlcNAcylation increases ChREBP protein content and transcriptional activity in the liver. Diabetes 60 (2011) 1399-1413.

[49]W. Xu, X. Zhang, J.L. Wu, L. Fu, K. Liu, D. Liu, G.G. Chen, P.B. Lai, N. Wong, J. Yu, O-GlcNAc transferase promotes fatty liver-associated liver cancer through inducing palmitic acid and activating endoplasmic reticulum stress. Journal of hepatology 67 (2017) 310-320.

[50]C. Phoomak, A. Silsirivanit, C. Wongkham, B. Sripa, A. Puapairoj, S. Wongkham, Overexpression of O-GlcNAc-transferase associates with aggressiveness of mass-forming cholangiocarcinoma. Asian Pac J Cancer Prev 13 Suppl (2012) 101-105.

[51]C. Phoomak, K. Vaeteewoottacharn, K. Sawanyawisuth, W. Seubwai, C. Wongkham, A. Silsirivanit, S. Wongkham, Mechanistic insights of O-GlcNAcylation that promote progression of cholangiocarcinoma cells via nuclear translocation of NF-kappaB. Sci Rep 6 (2016) 27853.

[52]Z. Qiao, C. Dang, B. Zhou, S. Li, W. Zhang, J. Jiang, J. Zhang, R. Kong, Y. Ma, O-linked N-acetylglucosamine transferase (OGT) is overexpressed and promotes O-linked protein glycosylation in esophageal squamous cell carcinoma. J Biomed Res 26 (2012) 268-273.

[53]T.J. Jang, U.J. Kim, O-GlcNAcylation is associated with the development and progression of gastric carcinoma. Pathol Res Pract 212 (2016) 622-630.

[54]Y.U. Cheng, H. Li, J. Li, J. Li, Y. Gao, B. Liu, O-GlcNAcylation enhances anaplastic thyroid carcinoma malignancy. Oncol Lett 12 (2016) 572-578.

[55]A. Steenackers, S. Olivier-Van Stichelen, S.F. Baldini, V. Dehennaut, R.A. Toillon, X. Le Bourhis, I. El Yazidi-Belkoura, T. Lefebvre, Silencing the Nucleocytoplasmic O-GlcNAc Transferase Reduces Proliferation, Adhesion, and Migration of Cancer and Fetal Human Colon Cell Lines. Front Endocrinol (Lausanne) 7 (2016) 46.

[56] T.J. Jang, Differential membranous E-cadherin expression, cell proliferation and O-GlcNAcylation between primary and metastatic nodal lesion in colorectal cancer. Pathol Res Pract 212 (2016) 113-119.

[57] M. Jiang, B. Xu, X. Li, Y. Shang, Y. Chu, W. Wang, D. Chen, N. Wu, S. Hu, S. Zhang, M. Li, K. Wu, X. Yang, J. Liang, Y. Nie, D. Fan, O-GlcNAcylation promotes colorectal cancer metastasis via the miR-101-O-GlcNAc/EZH2 regulatory feedback circuit. Oncogene 38 (2019) 301-316.

[58] H. Guo, B. Zhang, A.V. Nairn, T. Nagy, K.W. Moremen, P. Buckhaults, M. Pierce, O-Linked N-Acetylglucosamine (O-GlcNAc) Expression Levels Epigenetically Regulate Colon Cancer Tumorigenesis by Affecting the Cancer Stem Cell Compartment via Modulating Expression of Transcriptional Factor MYBL1. J Biol Chem 292 (2017) 4123-4137.

[59] L.V. Pham, J.L. Bryant, R. Mendez, J. Chen, A.T. Tamayo, Z.Y. Xu-Monette, K.H. Young, G.C. Manyam, D. Yang, L.J. Medeiros, R.J. Ford, Targeting the hexosamine biosynthetic pathway and O-linked N-acetylglucosamine cycling for therapeutic and imaging capabilities in diffuse large B-cell lymphoma. Oncotarget (2016) 12413.

[60] A. Asthana, P. Ramakrishnan, Y. Vicioso, K. Zhang, R. Parameswaran, Hexosamine Biosynthetic Pathway Inhibition Leads to AML Cell Differentiation and Cell Death. Molecular cancer therapeutics 17 (2018) 2226-2237.

[61] Q. Zeng, R.X. Zhao, J. Chen, Y. Li, X.D. Li, X.L. Liu, W.M. Zhang, C.S. Quan, Y.S. Wang, Y.X. Zhai, J.W. Wang, M. Youssef, R. Cui, J. Liang, N. Genovese, L.T. Chow, Y.L. Li, Z.X. Xu, O-linked GlcNAcylation elevated by HPV E6 mediates viral oncogenesis. Proc Natl Acad Sci U S A 113 (2016) 9333-9338.

[62] M. Kim, Y.S. Kim, H. Kim, M.Y. Kang, J. Park, D.H. Lee, G.S. Roh, H.J. Kim, S.S. Kang, G.J. Cho, J.K. Park, J.W. Cho, J.K. Shin, W.S. Choi, O-linked N-acetylglucosamine transferase promotes cervical cancer tumorigenesis through human papillomaviruses E6 and E7 oncogenes. Oncotarget 7 (2016) 44596-44607.

[63] G. Yehezkel, L. Cohen, A. Kliger, E. Manor, I. Khalaila, O-linked beta-N-acetylglucosaminylation (O-GlcNAcylation) in primary and metastatic colorectal cancer clones and effect of N-acetyl-beta-D-glucosaminidase silencing on cell phenotype and transcriptome. J Biol Chem 287 (2012) 28755-28769.

[64] Y. Niu, Y. Xia, J. Wang, X. Shi, O-GlcNAcylation promotes migration and invasion in human ovarian cancer cells via the RhoA/ROCK/MLC pathway. Molecular medicine reports 15 (2017) 2083-2089.

[65] S.B. Harosh-Davidovich, I. Khalaila, O-GlcNAcylation affects beta-catenin and E-cadherin expression, cell motility and tumorigenicity of colorectal cancer. Experimental cell research 364 (2018) 42-49.

[66]B. Zhang, P. Zhou, X. Li, Q. Shi, D. Li, X. Ju, Bitterness in sugar: O-GlcNAcylation aggravates pre-B acute lymphocytic leukemia through glycolysis via the PI3K/Akt/c-Myc pathway. American journal of cancer research 7 (2017) 1337-1349.

[67]R.M. de Queiroz, R. Madan, J. Chien, W.B. Dias, C. Slawson, Changes in O-Linked N-Acetylglucosamine (O-GlcNAc) Homeostasis Activate the p53 Pathway in Ovarian Cancer Cells. J Biol Chem 291 (2016) 18897-18914.

[68]S. Luanpitpong, N. Chanthra, M. Janan, J. Poohadsuan, P. Samart, U.P. Y, Y. Rojanasakul, S. Issaragrisil, Inhibition of O-GlcNAcase Sensitizes Apoptosis and Reverses Bortezomib Resistance in Mantle Cell Lymphoma through Modification of Truncated Bid. Molecular cancer therapeutics 17 (2018) 484-496.

[69]Y. Fardini, V. Dehennaut, T. Lefebvre, T. Issad, O-GlcNAcylation: A New Cancer Hallmark? Front Endocrinol (Lausanne) 4 (2013) 99.

[70] S.D. Lyons, M.E. Sant, R. I. Christopherson. Cytotoxic mechanisms of glutamine antagonists in mouse L1210 leukemia, Journal of Biological Chemistry 265 (1990):11377-11381.

[71] J.G. Moloughney, P.K. Kim, N. M. Vega-Cotto, C.C. Wu, S. Zhang, M. Adlam, T. Lynch, P. C., J. D. Rabinowitz, G. Werlen, E. Jacinto. mTORC2 Responds to Glutamine Catabolite Levels to Modulate the Hexosamine Biosynthesis Enzyme GFAT1. Molecular Cell 63 (2016): 811-826.
[72] a.K.Y. Christopher T. Saeui. Small molecular inhibitors of the hexosamine biosynthetic pathway and the cancer O-GlcNAcome [abstract], Cancer Research 76 (14 Supplement) (2016.)

[73]R. Trapannone, K. Rafie, D.M. van Aalten, O-GlcNAc transferase inhibitors: current tools and future challenges. Biochem Soc Trans 44 (2016) 88-93.

[74]R.F. Ortiz-Meoz, J. Jiang, M.B. Lazarus, M. Orman, J. Janetzko, C. Fan, D.Y. Duveau, Z.W. Tan, C.J. Thomas, S. Walker, A small molecule that inhibits OGT activity in cells. ACS Chem Biol 10 (2015) 1392-1397.

[75]Z. Wang, K. Park, F. Comer, L.C. Hsieh-Wilson, C.D. Saudek, G.W. Hart, Site-specific GlcNAcylation of human erythrocyte proteins: potential biomarker(s) for diabetes. Diabetes 58 (2009) 309-317.

[76]C. Springhorn, T.E. Matsha, R.T. Erasmus, M.F. Essop, Exploring leukocyte O-GlcNAcylation as a novel diagnostic tool for the earlier detection of type 2 diabetes mellitus. J Clin Endocrinol Metab 97 (2012) 4640-4649.

[77]W. Mi, Y. Gu, C. Han, H. Liu, Q. Fan, X. Zhang, Q. Cong, W. Yu, O-GlcNAcylation is a novel regulator of lung and colon cancer malignancy. Biochim Biophys Acta 1812 (2011) 514-519.

[78]S. Kanwal, Y. Fardini, P. Pagesy, T. N'Tumba-Byn, C. Pierre-Eugene, E. Masson, C. Hampe, T. Issad, O-GlcNAcylation-inducing treatments inhibit estrogen receptor alpha expression and confer resistance to 4-OH-tamoxifen in human breast cancer-derived MCF-7 cells. PLoS One 8 (2013) e69150.

[79]A. Golks, D. Guerini, The O-linked N-acetylglucosamine modification in cellular signalling and the immune system. 'Protein modifications: beyond the usual suspects' review series. EMBO Rep 9 (2008) 748-753.

[80]A. Golks, T.T. Tran, J.F. Goetschy, D. Guerini, Requirement for O-linked N-acetylglucosaminyltransferase in lymphocytes activation. Embo J 26 (2007) 4368-4379.

[81]L.R. James, D. Tang, A. Ingram, H. Ly, K. Thai, L. Cai, J.W. Scholey, Flux through the hexosamine pathway is a determinant of nuclear factor kappaB- dependent promoter activation. Diabetes 51 (2002) 1146-1156.

[82]N.S. Sharma, V.K. Gupta, V.T. Garrido, R. Hadad, B.C. Durden, K. Kesh, B. Giri, A. Ferrantella, V. Dudeja, A. Saluja, S. Banerjee, Targeting tumor-intrinsic hexosamine biosynthesis sensitizes pancreatic cancer to anti-PD1 therapy. The Journal of clinical investigation 130 (2020) 451-465.

[83]R.D. Leone, L. Zhao, J.M. Englert, I.M. Sun, M.H. Oh, I.H. Sun, M.L. Arwood, I.A. Bettencourt, C.H. Patel, J. Wen, A. Tam, R.L. Blosser, E. Prchalova, J. Alt, R. Rais, B.S. Slusher, J.D. Powell, Glutamine blockade induces divergent metabolic programs to overcome tumor immune evasion. Science 366 (2019) 1013-1021.

[84]L. Tardio, J. Andres-Bergos, N.E. Zachara, A. Larranaga-Vera, C. Rodriguez-Villar, G. Herrero-Beaumont, R. Largo, O-linked N-acetylglucosamine (O-GlcNAc) protein modification is increased in the cartilage of patients with knee osteoarthritis. Osteoarthritis Cartilage 22 (2014) 259-263.

[85]P.J. Lund, J.E. Elias, M.M. Davis, Global Analysis of O-GlcNAc Glycoproteins in Activated Human T Cells. J Immunol 197 (2016) 3086-3098.

[86]M. Swamy, S. Pathak, K.M. Grzes, S. Damerow, L.V. Sinclair, D.M. van Aalten, D.A. Cantrell, Glucose and glutamine fuel protein O-GlcNAcylation to control T cell self-renewal and malignancy. Nat Immunol 17 (2016) 712-720.

[87]M.B. Lazarus, Y. Nam, J. Jiang, P. Sliz, S. Walker, Structure of human O-GlcNAc transferase and its complex with a peptide substrate. Nature 469 (2011) 564-567.

[88]N.L. Elsen, S.B. Patel, R.E. Ford, D.L. Hall, F. Hess, H. Kandula, M. Kornienko, J. Reid, H. Selnick, J.M. Shipman, S. Sharma, K.J. Lumb, S.M. Soisson, D.J. Klein, Insights into activity and inhibition from the crystal structure of human O-GlcNAcase. Nature chemical biology 13 (2017) 613-615.

[89]S. Ruegenberg, M. Horn, C. Pichlo, K. Allmeroth, U. Baumann, M.S. Denzel, Loss of GFAT-1 feedback regulation activates the hexosamine pathway that modulates protein homeostasis. Nat Commun 11 (2020) 687.

 [90]JM Llovet, J Zucman-Rossi, E Pikarsky, B Sangro, M Schwartz, M Sherman, G Gores. Hepatocellular carcinoma. Nat Rev Dis Primers (2016) 2:16018.

[91]International Agency for Research on Cancer, World Health Organization. Cancer today (https://gco.iarc.fr/today/home.)

[92]American Cancer Society. Liver cancer survival rates (https://www.cancer.org/cancer/liver-cancer/detection-diagnosis-staging/survival-rates.html.)

[93]Ju et al. Int J Cancer 2015.

[94]TK Lee, RT Poon, AP Yuen, MT Ling, WK Kwok, XH Wang, YC Wong, XY Guan, K Man, KL Chau, ST Fan. Twist overexpression correlates with hepatocellular carcinoma metastasis through induction of epithelial-mesenchymal transition. Clin Cancer Res. (2006) 12(18):5369-76.

[95]CM Shachaf, AM Kopelman, C Arvanitis, A Karlsson, S Beer, S Mandl, MH Bachmann, AD Borowsky, B Ruebner, RD Cardiff, Q Yang, JM Bishop, CH Contag, DW Felsher. MYC inactivation uncovers pluripotent differentiation and tumour dormancy in hepatocellular cancer. Nature (2004) 431(7012):1112-7.

[96]R Dhanasekaran, V Baylot, M Kim, S Kuruvilla, DI Bellovin, N Adeniji, A Rajan Kd, I Lai, M Gabay, L Tong, M Krishnan, J Park, T Hu, MA Barbhuiya, AJ Gentles, K Kannan, PT Tran, DW Felsher. MYC and Twist1 cooperate to drive metastasis by eliciting crosstalk between cancer and innate immunity. Elife (2020) 9:e50731.

[97]D Massberg, A Simon, D Haussinger, V Keitel, G Gisselmann, H Conrad, H Hatt. Monoterpene (-)-citronellal affects hepatocarcinoma cell signaling via an olfactory receptor. Archives of biochemistry and biophysics (2015) 566, 100-109.

[98]RP Gajula, ST Chettiar, RD Williams, K Nugent, Y Kato, H Wang, R Malek, K Taparra, J Cades, A Annadanam, AR Yoon, E Fertig, BA Firulli, L Mazzacurati, TF Burns, AB Firulli, SS An, PT Tran. Structure-function studies of the bHLH phosphorylation domain of TWIST1 in prostate cancer cells. Neoplasia (2015) 17(1):16-31.

[99]NM Dalesio, SF Barreto Ortiz, JL Pluznick JL, DE Berkowitz. Olfactory, Taste, and Photo Sensory Receptors in Non-sensory Organs: It Just Makes Sense. Front Physiol (2018) 9:1673.

[100]JL Pluznick et al. Functional expression of the olfactory signaling system in the kidney. Proc Natl Acad Sci USA (2009) **106**, 2059–2064.

[101]C Flegel, S Manteniotis, S Osthold, H Hatt, G Gisselmann. Expression profile of ectopic olfactory receptors determined by deep sequencing. PLoS One (2013) **8**, e55368.

[102]X Zhang, O De la Cruz, JM Pinto, D Nicolae, S Firestein, Y Gilad. Characterizing the expression of the human olfactory receptor gene family using a novel DNA microarray. Genome Biol (2007) **8**, R86

[103]W Cao, F Li, J Yao, J Yu. Prostate specific G protein coupled receptor is associated with prostate cancer prognosis and affects cancer cell proliferation and invasion. BMC cancer (2015) 15, 915.

[104]EM Neuhaus, W Zhang, L Gelis, Y Deng, J Noldus, H Hatt. Activation of an olfactory receptor inhibits proliferation of prostate cancer cells. The Journal of biological chemistry (2009) 284, 16218-16225.

[105]T Braun, P Voland, L Kunz, C Prinz, M Gratzl. Enterochromaffin cells of the human gut: sensors for spices and odorants. Gastroenterology (2007) 132, 1890-1901.

[106]TY Chou, CV Dang, GW Hart. Glycosylation of the c-Myc transactivation domain. PNAS (1995) 92(10):4417-21.

[107]D Georgess, V Padmanaban, OK Sirka, K Coutinho, A Choi, G Frid, NM Neumann, T Inoue, AJ Ewald.
Twist1-Induced Epithelial Dissemination Requires Prkd1 Signaling. Cancer Res (2020) (2) 204-218.

[108]D Vigetti, S Deleonibus, P Moretto, E Karousou, M Viola, B Bartolini, VC Hascall, M Tammi, G De Luca, A Passi. Role of UDP-N-acetylglucosamine (GlcNAc) and O-GlcNAcylation of hyaluronan synthase 2 in the control of chondroitin sulfate and hyaluronan synthesis. J Biol Chem (2012) 287(42):35544-35555.

[109]PT Tran EH Shroff, TF Burns, S Thiyagarajan, ST Das, T Zabuawala, JChen, YJ Cho, R Luong, P Tamayo, T Salih, K Aziz, SJ Adam, S Vicent, CH Nielsen, N Withofs, A Sweet-Cordero, SS Gambhir, CM Rudin, DW Felsher. Twist1 Suppresses Senescence Programs and Thereby Accelerates and Maintains Mutant Kras-Induced Lung Tumorigenesis. PLoS Genet. **8,** e1002650 (2012.)

[110]BD Shepard, N Natarajan, RJ Protzko, OW Acres, JL Pluznick. A cleavable N-terminal signal peptide promotes widespread olfactory receptor surface expression in HEK293T cells. PLoS One (2013) 8(7):e68758.

[111]V Padmanaban, EM Grasset, NM Neumann, AK Fraser, E Henriet, W Matsui, PT Tran, KJ Cheung, D Georgess, AJ Ewald. Organotypic culture assays for murine and human primary and metastatic-site tumors. Nat Protoc (2020)15(8):2413-2442.

Curriculum Vitae

Christine Lam

PERSONAL INFORMATION
DOB: June 30, 1993
Citizenship: USA
E-mail: christineytlam@jhmi.edu

EDUCATION

DEGREE	INSTITUTION	DATE	FIELD
B.A.	University of California, Berkeley	2011–2015	Molecular and Cell Biology
Ph.D.	Johns Hopkins University School of Medicine	2017–2021 (exp)	Cellular and Molecular Medicine
M.D.	David Geffen School of Medicine at UCLA	2021–2025	Medicine

PROFESSIONAL POSITIONS

2012	Research Student, University of California, Berkeley, Dr. David Weisblat
2013	Research Student, National Cancer Centre Singapore (Singapore,) Dr. Kam Hui
2014–2015	Research Student, UC Berkeley, Dr. Kevin Healy
2015	Research Student, Infectious Diseases Research Collaboration (Uganda,) Dr. Philip Rosenthal
2015–2017	Research Specialist, University of California, San Francisco, Dr. Arun Wiita
2017	Ph.D. Student Research Rotation, Johns Hopkins University School of Medicine, Dr. Jennifer Elisseeff
2018	Ph.D. Student Research Rotation, JHU SOM, Dr. Donald Small
2018–2021	Ph.D. Graduate Student, JHU SOM Radiation Oncology, Dr. Phuoc Tran (Advisor)

AWARDS & HONORS
2012 Pre-Initiative for Maximizing Student Development Scholarship
2013 Benjamin A. Gilman International Scholarship
2013 Leadership Award
2014 Tung Sen Benevolent Association Scholarship
2014 Minority Health and Health Disparities International Research Training Fellowship
2019 National Science Foundation Graduate Research Fellowship
2020 Collaborative Teaching Fellowship

2018–   Haematologica
2019–   PLOS One
2020–   Journal of Clinical Investigation

PUBLICATIONS
1. Ronan Le Moigne, Blake T. Aftab, Stevan Djakovic, Eugen Dhimolea, Eduardo Valle, Megan Murnane, Emily M. King, Ferdie Soriano, Mary-Kamala Menon, Zhi Yong Wu, Stephen T. Wong, Grace J. Lee, Bing Yao, Arun P. Wiita, **Christine Lam**, Julie Rice, Jinhai Wang, Marta Chesi, P. Leif Bergsagel, Marianne Kraus, Christoph Driessen, Szerenke Kiss Von Soly, F. Michael Yakes, David Wustrow, Laura Shawver, Han-Jie Zhou, Thomas G. Martin III, Jeffrey L. Wolf, Constantine S. Mitsiades, Daniel J. Anderson, Mark Rolfe. The p97 inhibitor CB-5083 is a unique disrupter of protein homeostasis in models of multiple myeloma. *Molecular Cancer Therapeutics* 2017. 16(11):2375-2386.

2. **Christine Lam**, Ian D. Ferguson, Margarette C. Mariano, Yu-Hsiu T. Lin, Megan Murnane, Hui Liu, Geoffrey A. Smith, Sandy W. Wong, Jack Taunton, Jun O. Liu, Constantine S. Mitsiades, Byron C. Hann, Blake T. Aftab, Arun P. Wiita. Repurposing tofacitinib as an anti-myeloma therapeutic to reverse growth-promoting effects of the bone marrow microenvironment. *Haematologica* 2018. 103(7):1218-1228.

3. Ryan M. Phillips*, **Christine Lam*,** Hailun Wang, Phuoc T. Tran. Bittersweet tumor development and progression: Emerging roles of epithelial plasticity glycosylations. *Advances in Cancer Research* 2019. 142:23-62.

4. Hector H. Huang, Ian D. Ferguson, Alexis M. Thornton, Prabhakar Bastola, **Christine Lam**, Yu-Hsiu T. Lin, Priya Choudhry, Margarette C. Mariano, Makeba D. Marcoulis, Chin Fen Teo, Julia Malato, Paul J. Phojanakong, Thomas G. Martin III, Jeffrey L. Wolf, Sandy W. Wong, Nina Shah, Byron Hann, Angela N. Brooks, Arun P. Wiita. Proteasome inhibitor-induced modulation reveals the spliceosome as a specific therapeutic vulnerability in multiple myeloma. *Nature Communications* 2020. 11(1):1931.

5. **Christine Lam*,** Jin-Yih Low*, Wang H, Tran PT. Hexosamine biosynthesis pathway and cancer: current achievements and future therapeutic strategies. *Cancer Letters* 2021. 503(2021):11-18.

6. Xing Wang*, Natasha Raman*, Ghali Lemtiri-Chlieh*, Katriana Nugent, Matthew Ballew, Travis Peck, Michelle Levine, Audrey Lafargue, **Christine Lam**, Reem Malek, Ryan Phillips, Zhuo An Cheng, Kekoa Taparra, Michael Lim, Andrew Holland, Phuoc T. Tran, Hailun Wang. Centrosome clustering inhibition activates cGAS and radiosensitizes non-small cell lung cancer cells. *International Journal of Radiation Oncology, Biology, Physics.* Under review.

7. Ian D. Ferguson, Yu-Hsiu T. Lin*, **Christine Lam***, Hao Shao, Martina Hale, Kevin M. Tharp, Margarette C. Mariano, Veronica Steri, Donghui Wang, Paul Phojanokong, Sami T. Tuomivaara, Byron Hann, Christoph Driessen, Brian Van Ness, Jason E. Gestwicki, Arun P.

Wiita. Allosteric HSP70 inhibitors perturb mitochondrial proteostasis and overcome proteasome inhibitor resistance in multiple myeloma. *eLife.* Under review. (Pre-print: https://www.biorxiv.org/content/10.1101/2020.04.21.052456v1)

(*indicates equal contribution)

ABSTRACTS

1. **Christine Lam,** Sung-Jin Cho, David Weisblat. Transcript levels vary in a complementary manner at the two-cell stage in the leech *Helobdella austinensis.* University of California, Berkeley Biology Scholars Program Summer Undergraduate Research Symposium 2012. Berkeley, CA.

2. **Christine Lam,** Nikhil A. Rode, Min Ju Lee, Natalie C. Marks, Willie M. Reese, Kevin E. Healy. Biologically active hyaluronic acid-based electrospun matrices for cardiac repair. UC Berkeley Molecular and Cell Biology Honors Poster Session 2015. Berkeley, CA.

3. **Christine Lam,** Megan Murnane, Geoffrey A. Smith, Jack Taunton, Blake T. Aftab, Arun P. Wiita. Tofacitinib reverses growth promoting effects of the bone marrow stromal environment through JAK1/STAT3 signaling in multiple myeloma. University of California, San Francisco Cancer Center Conference 2016. Santa Cruz, CA.

4. **Christine Lam,** Megan Murnane, Geoffrey A. Smith, Jack Taunton, Blake T. Aftab, Arun P. Wiita. Tofacitinib reverses growth promoting effects of the bone marrow stromal environment through JAK1/STAT3 signaling in multiple myeloma. American Society of Hematology Annual Meeting 2016. San Diego, CA.

5. Hui Liu, **Christine Lam**, Bernd Jandeleit, Wolf-Nicolas Fisher, Kerry Koller, Byron Hann, Arun P. Wiita. Hijacking myeloma metabolism to target cytotoxic chemotherapy to malignant plasma cells with decreased bone marrow toxicity. International Myeloma Workshop 2017. New Delhi, India.

6. Hector H. Huang, **Christine Lam**, Alexis Thornton, Margarette C. Mariano, Ian D. Ferguson, Byron Hann, Angela N. Brooks, Arun P. Wiita. Unbiased phosphoproteomics reveals a therapeutically relevant connection between pre-mRNA splicing and proteasome inhibition in multiple myeloma. American Society of Hematology Annual Meeting 2017. Atlanta, GA.

8. Ian D. Ferguson, **Christine Lam**, Margarette C. Mariano, Donghui Wang, Paul Phojanokong, Sami T. Tuomivaara, Hao Shao, Byron Hann, Jason E. Gestwicki, Arun P. Wiita. Novel allosteric inhibitors of heat shock protein 70 as agents to probe protein homeostasis and overcome proteasome inhibitor resistance in multiple myeloma. American Society of Hematology Annual Meeting 2018. San Diego, CA.

9. **Christine Lam**, Colburn Yu, Ismaeel Siddiqui, Hailun Wang, Phuoc T. Tran. One-two punch of Twist1 inhibition and the senolytic ABT263 is an effective therapeutic strategy for non-small cell lung cancer. Radiation Oncology Scientific Retreat 2019. Baltimore, MD.

10. Francesca A. Carrieri, Nick Connis, Eloise M. Grasset, Isaac S. Chan, Eddie Luidy-Imada, **Christine Lam**, Hailun Wang, Andrew J. Ewald, Luigi Marchionni, Christine L. Hann and Phuoc T. Tran. Establishment of patient-derived organoids as *ex vivo* tool to characterize the molecular mechanisms of SCLC chemo-radiation resistance. American Association for Cancer Research 2020.

11. **Christine Lam**, Mustafa A. Barbhuiya, Michael Considine, Elodie Henriet, Hailun Wang, Francesca A. Carrieri, Audrey Lafargue, Caleb Smack, Ismaeel Siddiqui, Luciane T. Kagohara, Adam C. Mirando, Richard J. Sove, Mark Yarchoan, Aleksander S. Popel, Andrew J. Ewald, Elana J. Fertig, Phuoc T. Tran. Integrated transcriptomic and proteomic analyses reveal role of the hexosamine biosynthetic pathway in invasion and metastasis of hepatocellular carcinoma. **Oral presentation** in Biology 05 Session of the American Society of Radiation Oncology Annual Meeting 2020.

12. Caleb R.P. Smack, Audrey Lafargue, Christine Lam, Francesca A. Carrieri, Ismaeel Siddiqui, Hailun Wang and Phuoc T. Tran. he harmala alkaloid harmine as a novel cancer cell radiosensitizer. AACR Virtual Special Conference on Radiation Science and Medicine 2021.

13. Audrey Lafargue, Hailun Wang, Sivarajan T. Chettiar, Rajendra P. Gajula, Caleb Smack, Ismaeel Siddiqui, Kekoa Taparra, Christine Lam, Francesca Carrieri, Katriana Nugent, Natasha Zachara and Phuoc T. Tran. The transactivation domain of TWIST1 is required for TWIST1-induced aggressiveness in non-small cell lung cancer. AACR Virtual Special Conference on Radiation Science and Medicine 2021.

ORAL PRESENTATIONS
1. Surveillance of antimalarial drug resistance in Tororo, Uganda. University of California, Berkeley Global Health Fellows Symposium 2015. Berkeley, CA.

2. Potential role of FLT3 in microcephaly. Johns Hopkins University School of Medicine Cellular and Molecular Medicine Rotation Presentations 2018. Baltimore, MD.

3. One-two punch of Twist1 inhibition and the senolytic ABT263 is an effective therapeutic strategy for non-small cell lung cancer. JHU SOM Brady Urological Institute Seminar 2018. Baltimore, MD.

4. One-two punch of Twist1 inhibition and the senolytic ABT263 is an effective therapeutic strategy for non-small cell lung cancer. JHU SOM Molecular Radiation Sciences Seminar 2018. Baltimore, MD.

5. Integrated transcriptomic and proteomic analyses reveal role of the hexosamine biosynthetic pathway in invasion and metastasis of hepatocellular carcinoma. JHU SOM Brady Urological Institute Seminar 2019. Baltimore, MD.

6. Integrated transcriptomic and proteomic analyses reveal role of the hexosamine biosynthetic pathway in invasion and metastasis of hepatocellular carcinoma. JHU SOM Molecular Radiation Sciences Seminar 2019. Baltimore, MD.

7. How to be successful in research. Society of Asian Scientists and Engineers Northeast Regional Conference 2019. College Park, MD.

8. Integrated transcriptomic and proteomic analyses reveal role of the hexosamine biosynthetic pathway in invasion and metastasis of hepatocellular carcinoma. JHU SOM Sidney Kimmel Comprehensive Cancer Center Fellow Research Day 2020. Baltimore, MD.

9. Integrated transcriptomic and proteomic analyses reveal role of the hexosamine biosynthetic pathway in invasion and metastasis of hepatocellular carcinoma. JHU SOM Cancer Invasion and Metastasis Seminar 2021. Baltimore, MD.

RESEARCH SUPPORT
Pre-Initiative for Maximizing Student Development Scholarship
6/2012–8/2012
National Institutes of Health
$4,100

Benjamin A. Gilman International Scholarship   6/2013
U.S. Department of State
$5,000

Minority Health and Health Disparities International Research Training Fellowship
1/2015–9/2015
National Institutes of Health
$10,200

NSF Graduate Research Fellowship   6/2019–
National Science Foundation
$138,000

TEACHING
1. JHU Special Opportunities in Undergraduate Learning (Fall 2019.) "Mouse Models in Cancer Research."
   - **Teaching certificate from Johns Hopkins University Teaching Academy (2019)**
2. Baltimore Underground Science Space. "Bittersweet Tumor Development and Progression."
   - **Collaborative Teaching Fellowship (2020)**

LEADERSHIP & VOLUNTEERING

Reach the World, Travel Correspondent
2013
Worked with an underrepresented elementary school classroom in New York to develop the students' knowledge of Singapore and gain global competence in today's global community through weekly journalistic postings and video logs about my experiences traveling abroad to Singapore, Malaysia, and Thailand.

UC Berkeley Society of Asian Scientists and Engineers, President
2013–2015
Hosted info-sessions and professional development events with companies including Procter & Gamble, General Electric, Sandia National Labs, and Genentech to help members develop professionally and find internship, research, or job opportunities.
- **Leadership Award (2013)**
- **Most Influential Chapter Finalist (2015)**

Bay Area Scientists in Schools, Volunteer Science Teacher
2012–2015
Led hands-on science lesson presentations (DNA Discovery and Build-A-Bug lessons) for >300 students at under-resourced public elementary school lacking a proper science education program.

Southeast Health Center, Volunteer Medical Scribe
2016
Documented interactions between patient and provider and physical examination results on the electronic medical record. Assisted provider with writing discharge instructions, submitting patient referrals, and giving educational handouts to patients.

Johns Hopkins University Society of Asian Scientists and Engineers, Founder and President
2020–Established emotional intelligence program and mentorship programs. Planning professional development and networking events.

Johns Hopkins University Basic Science Institute, Near Peer Mentor
2020–Provided career-related mentorship to undergraduate students interested in biomedical careers. Led weekly journal clubs with students.

OCCUPATIONAL BACKGROUND
1. Research Specialist. University of California, San Francisco. 9/2015–7/2017.
2. College Admissions Counselor. Empowerly. 8/2018–4/2019.